Chapter 5

Experimental results and methodology for experimental validation

5.1 Introduction

In this chapter experimental results intended for experimental validation of numerical models of compact fin-and-tube heat exchangers and liquid overfeed refrigeration systems are presented (see chapter 2). The results have been obtained with the developed experimental infrastructure described in detail in chapter 3, following the procedures and formulation presented in chapter 4. The different facilities composing the experimental infrastructure permit experimentation of air-cooling compact heat exchangers using liquid refrigerant, and experiments with the liquid overfeed refrigeration system using the refrigerant R134a. Experiments on the refrigeration system are performed considering separately the different components and the system as a whole, permitting validation of the corresponding numerical models. In the developed experimental work special attention has been paid to the assessment of the experimental uncertainty and the experimental verification through energy balance checks, as an essential pre-requisite for the validation. For example, in the tests of the air-cooling compact heat exchangers the cooling capacities determined independently on both air- and refrigerant-side have been compared. A methodology for experimental validation of numerical models of compact heat exchangers is developed and proposed. The methodology is based on systematic comparisons of numerical with experimental results, and has been illustrated with the available data. In the experiments with the refrigerant system heat balance checks have been done for the major components of the system in order to verify the correctness of the results.

5.2 Data presentation

The results presented in this chapter deal with prototypes of heat exchangers using liquid refrigerant, liquid overfeed evaporators and the vapour-compression refrigeration system. More specifically, section 5.3 is dedicated to experiments with a copper-aluminium heat exchanger, and section 5.4 to experiments with a galvanized steel heat exchanger, both using liquid refrigerant. Section 5.5 deals with the liquid overfeed refrigeration systems, and the detailed study of the evaporator. The structure of the sections 5.3 and 5.4 is similar, with the information presented in the following order. Detailed description of the test prototype is given, with information about the materials used for fabrication, the tube arrangement, dimensions, geometry, configuration of the refrigerant circuits, etc. The average values of the measured variables during the experiment in steady state conditions are presented in tabular form. The calculated from them variables, together with their respective uncertainties are presented subsequently. The cooling capacities are determined following the methodology exposed in detail in section 4.4. The uncertainty analysis formulation and considerations are exposed in section 4.5. The stated as experimental cooling capacity is the averaged of the cooling capacities measured air- and refrigerant-side:

$$\dot{Q}_{exp} = 0.5(\dot{Q}_a + \dot{Q}_r) \tag{5.1}$$

The uncertainty of the experimental cooling capacity is obtained as an uncertainty of the result ($\dot{Q}_{exp}$) obtained from equation 5.1, having two variables: ($\dot{Q}_a$) and ($\dot{Q}_r$). The uncertainty propagation equation is in a similar form as that used for the random uncertainty, equation (4.26), and gives as a result:

$$U_{exp} = 0.5[{U_a}^2 + {U_r}^2]^{1/2} \tag{5.2}$$

In order to be verified for correctness the experimental results, energy balance checks have been done for the tested heat exchanger. The cooling capacities determined independently on both air- and refrigerant-side have been represented graphically with plotted ranges of experimental uncertainties. Correct experimental results must agree within the range of the expected uncertainty intervals. In the execution phase of the experiment, such a verification permits to control the experimental quality, and to detect unexpected instrument or measured process control failure.
A methodology for experimental validation of fin-and-tube heat exchanger models is proposed and illustrated, based on systematic comparisons of numerical and experimental results for the different prototypes and their statistical analysis. The numerical results are compared to experimental results in four aspects: heat transfer, pressure loss air-side, pressure loss refrigerant-side, and water vapour condensed rate over the fins and tubes of the heat exchanger for the wet cases. The numerical to experimental comparisons have been performed using an especially developed code (see section 4.7

for details).
Statistical analysis has been carried out in order to determine the average difference and its respective dispersion for the compared cases. In order to test in more detail the abilities of the numerical model to predict the real behaviour of the equipment, the test cases have been studied as a whole, and divided in four groups according to air velocity, refrigerant velocity (or flow-rate), dry and wet cases. This would reveal if some relation exists between the numerical-experimental differences and some specific working conditions, and would prove the range and capabilities of the model to predict the real phenomena. For each statistically analysed group of compared cases the average experimental uncertainty is calculated as $\bar{U}_{exp} = \frac{1}{N}\sum U_{exp}$, indicating the level of accuracy to which the numerical-experimental differences can be considered, interpreted, and conclusions about them be made.
The numerical to experimental average difference $\bar{\delta}$, the average absolute difference $|\bar{\delta}|$ and their respective standard deviations are calculated from the equations:

$$\delta = \frac{\phi_{num} - \phi_{exp}}{\phi_{exp}}.100, \quad [\%] \tag{5.3}$$

$$\bar{\delta} = \frac{1}{N}\sum_{i=1}^{N}\Big(\frac{\phi_{num} - \phi_{exp}}{\phi_{exp}}\Big).100, \quad [\%] \tag{5.4}$$

$$|\bar{\delta}| = \frac{1}{N}\sum_{i=1}^{N}\Big|\frac{\phi_{num} - \phi_{exp}}{\phi_{exp}}\Big|.100, \quad [\%] \tag{5.5}$$

$$S_{\delta} = \left[\frac{1}{N-1}\sum_{i=1}^{N}(\delta - \bar{\delta})^2\right]^{\frac{1}{2}}, \quad [\%] \tag{5.6}$$

$$S_{|\delta|} = \left[\frac{1}{N-1}\sum_{i=1}^{N}(|\delta| - |\bar{\delta}|)^2\right]^{\frac{1}{2}}, \quad [\%] \tag{5.7}$$

where ϕ can be the cooling capacity, the air-side pressure drop, the refrigerant-side pressure drop or the water vapour condensed rate in wet cases.
Finally, graphical numerical to experimental comparisons are presented, permitting visual evaluation of the comparative results.

Section 5.5 of this chapter is dedicated to the liquid overfeed refrigeration system as a whole and more specifically to the detailed analysis of the evaporator. The experimental facility permits two modes of working with phase-changing refrigerant, as explained in chapter 3. The first mode is experimentation with the vapour-compression cycle, measuring temperatures, pressures and flow-rates necessary for its experimental characterization, and obtaining of results for the basic components of

the system, that can be used for validation of numerical models. The second mode of experimentation is using the circuit without compressor, intended for separate testing of the liquid overfeed evaporator. The experimental results from the measurements of the variables in the phase-changing refrigerant circuit, and the secondary fluids in the evaporator and the condenser are presented, for both modes of working of the facility. Heat balance checks for the basic components of the refrigeration cycle are performed. The compressor work is determined experimentally and compared with manufacturer data. Detailed study of the liquid overfeed evaporator is carried out. Its cooling capacity has been determined experimentally using the methodology described in chapter 4. An illustrative experimental validation for the evaporator is presented, using the data obtained from the testing with the refrigeration cycle and the tests without compressor. The validation methodology follows similar procedure as the used for the compact heat exchangers with liquid refrigerant.

5.3 Copper-aluminium heat exchanger

A prototype of air-cooling compact heat exchanger, working with liquid refrigerant, has been experimentally tested using the developed experimental infrastructure. Detailed description of the experimental infrastructure is presented in sections 3.2 and 3.3. Description of the measuring instrumentation is given in section 3.5.
The heat exchanger prototype is fabricated from copper tubes and aluminium fins. The contact between the tubes and the fins is assured through a mechanical expansion of the tubes, which is the industrially used technology for fabrication of this type of equipment. The arrangement of the tubes is staggered for the consecutive rows. The aluminium fins have wavy form, used for enhancement of the heat transfer air-side. The geometry of the tubes and the fins is represented schematically in Figure 5.1. The exact values of the geometrical parameters are presented in Table 5.1.
The prototype has been constructed with a frame facilitating its coupling with the air-handling circuit (section 3.2), where is mounted between short duct sections guiding the air through the heat exchanger and permitting the mounting of the necessary instrumentation. A drawing of the test prototype is presented in Figure 5.3. A scheme of the test section air-side with the instrumentation is presented in section 3.5.1.
The heat exchanger prototype has been experimentally tested using pure water as a refrigerant, connected to the liquid refrigerant circuit (section 3.3). The cold water passing through the heat exchanger is distributed in four circuits by means of vertical collectors. Each refrigerant circuit consists of 8 tubes. The arrangement of the refrigerant circuits through the test prototype is presented in Figure 5.2.
The inlet and outlet refrigerant temperatures are measured with RTD, Pt100, and the refrigerant mass flow-rate is measured with Coriolis effect mass flow-meter. The instrument accuracies are given in section 3.5.2.

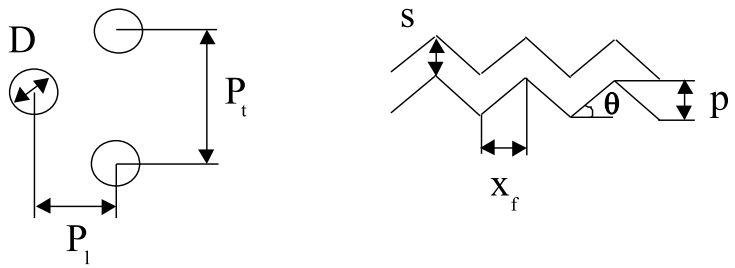

Figure 5.1: Geometry of the heat exchanger's tubes and fins

Model	Cu-Al
Tubes' arrangement	Staggered
Number of tubes in depth (X)	4
Number of tubes in height (Y)	8
Number of circuits	4
Longitude of fins in X[mm]	136
Longitude of fins in Y[mm]	304
Longitude of the heat exchanger in Z[mm]	410
Tube distance in X (P_l)[mm]	34
Tube distance in Y (P_t)[mm]	38
Material of fins	Aluminium
Fin pitch (s)[mm]	2.5
Fin thickness [mm]	0.12
Type of fin	Wavy
Semi-longitude of fin wave (x_f)[mm]	8.5
Amplitude of fin wave (p)[mm]	1.2
Fin angle (θ)[degrees]	8
Material of tube	Copper
Exterior diameter of tube [mm]	16.25
Tube thickness [mm]	0.4

Table 5.1: Cu-Al prototype definition

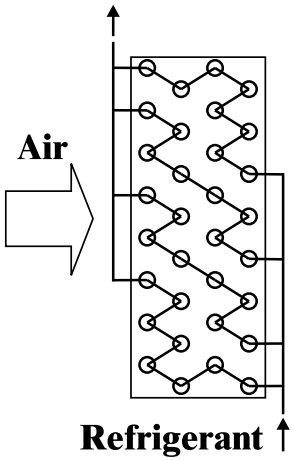

Figure 5.2: Refrigerant circuitry

The prototype has been prepared for measurement of the liquid refrigerant pressure loss, with pressure takes installed, permitting the measurement of the total refrigerant pressure loss through the heat exchanger (with inlet and outlet collector), and through a single refrigerant circuit. The mounting of the differential pressure transducer is shown in Figure 3.15, (section 3.5.2).
The air temperatures have been measured at the inlet and outlet transversal sections with 4 thermo-couples respectively, collocated at a distance of 700 mm before and after the prototype. The air pressure loss through the tested prototype is measured with differential pressure transducer, sensing the pressure at the inlet and outlet sections of the heat exchanger through four small taps in the centre of the duct walls in each section, connected to an equalizing piezometric ring conducting the sensed pressure to the transducer.

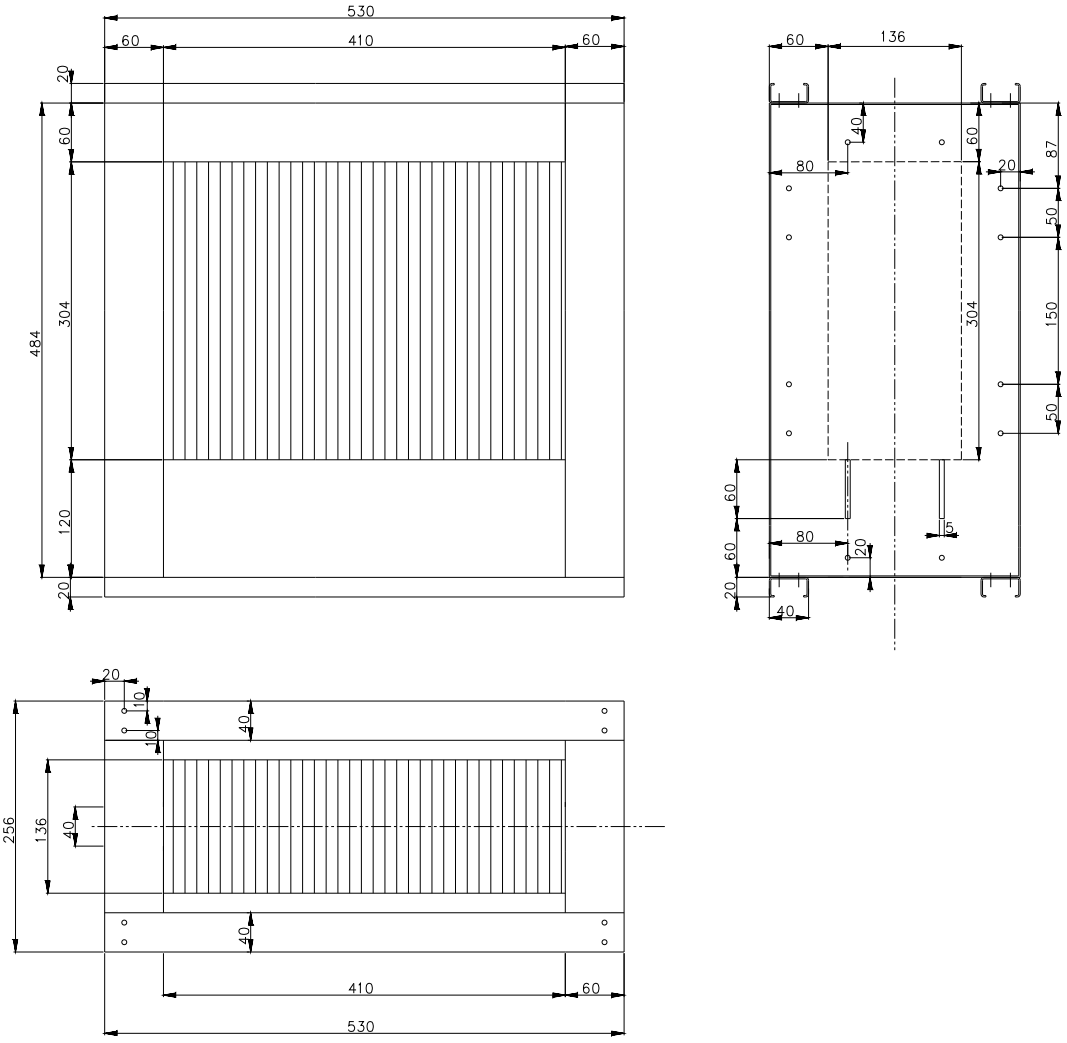

Figure 5.3: Construction and dimensions of the copper-aluminium prototype

5.3.1 Experimental results

The experiments with the air-cooling copper-aluminium heat exchanger prototype have been performed with the facility running in stable conditions. The range of working conditions comprises air velocities between 1.5 and 4 m/s, refrigerant velocities inside the heat exchanger's tubes between 0.5 and 2 m/s, with inlet relative air humidities from approximately 20 to 85 %. The inlet air temperature range is from approximately 18 to 32^{o}C. The refrigerant inlet temperature have been maintained at 7^{o}C. The experimental data consists of 64 tests, of which 18 are performed in dry conditions, and the rest 46 are wet tests (with water vapour condensation over the fins air-side).

The variables necessary for the determining of the cooling capacity of the prototype independently on the air- and refrigerant-side are measured. On the air side the air mass flow-rate and inlet and outlet air temperatures and relative humidities have been measured. For the wet experimental cases the condensed water flux over the fins of the tested heat exchanger is measured in order to determine the latent cooling load over the prototype. The relative humidity is measured with capacitance type sensors, and due to the decrease of accuracy of these type of sensors in near saturation conditions ($\varphi > 90\%$), the relative humidity at the outlet has been calculated from the relative humidity at the inlet, the condensate flux and the air temperatures at the inlet and outlet using psychrometrical relations. The air pressure loss through the heat exchanger is also measured.

On the refrigerant-side the refrigerant flow-rate and the inlet and outlet refrigerant temperatures are measured. The refrigerant pressure loss is measured with differential pressure transducer. The measured variables are presented in Table 5.2.

From the measured experimental variables the air and refrigerant velocities, the the air- and refrigerant-side cooling capacities, and their respective uncertainty intervals have been calculated. The cooling capacities have been calculated using the formulation presented in sections 4.4.1 and 4.4.2 respectively. The analysis of propagation of the individual measurements' uncertainties to the uncertainty of the cooling capacity has been evaluated using the formulation and the methodology presented in section 4.5. The stated as experimental cooling capacity ($\dot{Q}_{exp}$) is obtained as an arithmetic mean of the cooling capacities determined air- and refrigerant-side, with uncertainty calculated from equation 5.2. As an estimation of the agreement between the cooling capacities determined on both sides, the difference between them have been calculated relative to the experimental cooling capacity. The calculated variables and results are presented in Table 5.3.

The experimental uncertainties obtained for the cooling capacities are, in general, higher for the capacities determined from the refrigerant-side. This is due to the low temperature lift in the refrigerant through the heat exchanger, because of its particular design and short refrigerant circuits.

Case	$\dot{m}_a$ $[\frac{kg}{s}]$	T_{ai} $[C]$	T_{ao} $[C]$	φ_i [%]	$\varphi_o{}^*$ [%]	P_{apl}^{exp} $[Pa]$	$\dot{m}_{cond}$ $[\frac{kg}{h}]$	$\dot{m}_r$ $[\frac{kg}{h}]$	T_{ri} $[C]$	T_{ro} $[C]$	P_{rpl}^{exp} $[Pa]$
1	0.2307	32.13	13.88	21.14	63.90	25.4	0.000	1375	7.00	9.63	2246
2	0.2148	27.01	11.34	31.95	84.93	25.5	0.000	2703	7.00	8.09	7798
3	0.2101	28.89	11.28	27.80	82.80	26.8	0.000	4064	7.00	7.81	16400
4	0.2168	31.70	11.82	22.82	77.02	24.2	0.000	5413	7.00	7.71	27750
5	0.2880	25.73	13.34	37.18	80.32	44.8	0.000	1359	6.99	9.27	2164
6	0.2878	27.10	12.69	33.05	80.77	44.5	0.000	2702	7.00	8.33	7778
7	0.2839	27.75	12.38	31.45	81.47	45.1	0.000	4052	6.99	7.93	16280
8	0.2818	28.93	12.36	29.60	82.21	45.5	0.000	5426	7.00	7.77	27830
9	0.2791	29.36	12.45	28.72	81.37	46.4	0.000	5422	7.00	7.78	27780
10	0.4442	25.78	15.38	38.59	73.25	90.2	0.000	1355	7.00	9.91	2163
11	0.4271	31.18	15.73	22.99	58.37	74.4	0.000	2700	7.00	9.06	7699
12	0.4417	25.47	13.55	36.08	75.65	92.9	0.000	4045	6.99	8.11	16010
13	0.4362	25.80	13.27	35.64	77.61	94.9	0.000	5427	6.99	7.86	27800
14	0.4356	25.44	13.17	35.83	76.87	95.3	0.000	5425	7.00	7.87	27790
15	0.5686	30.72	18.86	23.32	47.31	121.6	0.000	1372	7.00	11.14	2212
16	0.5912	24.07	14.78	41.34	73.57	145.0	0.000	2698	7.00	8.75	7755
17	0.5910	24.44	14.42	39.21	73.02	148.9	0.000	4039	7.01	8.27	15900
18	0.5770	27.96	15.25	27.60	60.04	123.2	0.000	5401	7.00	8.16	27570
19	0.2717	23.31	13.72	64.38	95.93	65.5	2.120	1361	7.00	9.59	2271
20	0.2718	23.48	13.89	65.35	96.30	65.5	2.280	1361	7.00	9.66	2275
21	0.2721	23.35	13.78	64.59	96.31	65.4	2.120	1361	7.00	9.60	2279
22	0.2693	23.52	14.64	74.53	97.09	65.9	3.400	1357	7.00	10.02	2277
23	0.2698	23.49	14.69	74.97	96.66	65.9	3.480	1356	7.00	10.06	2261
24	0.2694	23.49	14.63	74.50	97.12	65.9	3.380	1356	7.00	10.02	2266
25	0.2691	23.52	15.09	79.89	97.51	65.2	4.040	1357	7.00	10.24	2266
26	0.2698	23.27	14.96	80.35	98.04	65.1	3.940	1357	7.00	10.20	2271
27	0.2712	22.92	14.80	80.73	97.94	64.4	3.840	1357	7.00	10.13	2273
28	0.2734	22.42	14.49	80.67	98.51	63.7	3.580	1359	7.00	9.99	2289
29	0.2993	23.52	12.59	55.04	93.54	80.8	1.600	2705	7.00	8.42	7995
30	0.3023	23.69	12.77	55.67	94.05	80.5	1.695	2705	7.00	8.45	7968
31	0.3007	23.57	12.57	54.32	93.66	80.6	1.490	2706	7.00	8.41	7988
32	0.2894	21.12	11.76	64.26	94.57	63.9	2.023	2704	7.00	8.31	7766
33	0.2898	21.94	12.24	64.76	94.14	62.8	2.427	2703	7.00	8.44	7765
34	0.2898	21.28	11.88	64.77	94.44	63.5	2.160	2703	7.00	8.34	7767
35	0.2865	23.44	13.65	75.03	92.84	63.5	4.731	2702	6.99	8.93	7712
36	0.2865	22.96	13.38	75.02	93.61	63.4	4.412	2702	7.02	8.86	7722
37	0.2941	22.59	13.82	79.92	93.65	81.6	4.860	2729	7.00	8.90	8016
38	0.2931	22.71	14.02	81.06	94.04	81.1	5.000	2728	7.00	8.94	7914
39	0.2944	22.72	13.91	80.05	94.33	81.7	4.881	2727	7.00	8.91	7931
40	0.2956	22.53	13.74	79.36	93.39	81.3	4.800	2730	6.99	8.88	8037
41	0.2953	22.66	13.84	78.91	94.63	80.3	4.629	2729	6.99	8.87	7937
42	0.2843	23.56	14.44	84.66	95.51	63.7	5.876	2698	7.28	9.41	7678
43	0.4220	20.40	13.52	64.56	91.92	122.7	1.180	1362	7.00	9.35	2192
44	0.4204	20.09	13.31	64.47	91.78	123.2	1.090	1361	7.00	9.27	2212
45	0.4123	21.30	14.92	74.95	94.25	124.4	2.856	1359	7.00	10.00	2185
46	0.4081	21.47	14.95	74.74	93.70	126.4	3.029	1360	7.01	10.05	2175
47	0.4107	22.45	15.53	75.48	96.36	133.7	3.360	1358	7.00	10.25	2303
48	0.4124	22.16	15.30	75.00	96.45	133.3	3.120	1355	7.00	10.16	2256
49	0.4030	23.12	16.38	79.64	96.92	135.9	4.231	1356	7.01	10.64	2250
50	0.4032	23.34	16.51	79.32	96.26	135.8	4.400	1355	7.00	10.68	2244
...	...	...	...	...	...	...	...	...	...	...	...
64	0.4178	20.23	13.20	79.97	94.65	135.3	4.460	4100	7.00	8.28	16390
*	φ_o is calculated from the other results										

Table 5.2: Measured experimental results

Case	V_a	V_r	$\dot{Q}_a$	U_a	$\dot{Q}_r$	U_r	$\dot{Q}^*_{exp}$	U_{exp}	$100\frac{\lvert\dot{Q}_a-\dot{Q}_r\rvert}{\dot{Q}_{exp}}$
	$[m/s]$	$[m/s]$	$[W]$	[%]	$[W]$	[%]	$[W]$	[%]	[%]
1	1.63	0.51	4259	±3.17	4221	±4.41	4240	±2.71	0.90
2	1.51	1.00	3406	±3.58	3421	±10.47	3414	±5.54	0.44
3	1.48	1.50	3744	±3.35	3808	±14.11	3776	±7.30	1.69
4	1.53	2.00	4359	±3.03	4460	±16.03	4410	±8.25	2.26
5	2.01	0.50	3612	±4.26	3609	±5.06	3611	±3.31	0.07
6	2.02	1.00	4197	±3.90	4188	±8.57	4193	±4.70	0.21
7	2.00	1.50	4415	±3.56	4434	±12.09	4425	±6.31	0.44
8	1.99	2.00	4724	±3.41	4876	±14.71	4800	±7.66	3.11
9	1.98	2.00	4779	±3.42	4929	±14.54	4854	±7.57	3.05
10	3.11	0.50	4678	±4.64	4600	±4.01	4639	±3.07	1.71
11	3.01	1.00	6671	±3.46	6479	±5.59	6575	±3.26	2.96
12	3.09	1.49	5327	±4.19	5270	±10.17	5299	±5.48	1.07
13	3.05	2.01	5530	±4.04	5560	±12.91	5545	±6.78	0.53
14	3.04	2.00	5406	±4.11	5456	±13.15	5431	±6.91	0.92
15	3.99	0.51	6820	±4.22	6623	±2.91	6722	±2.58	2.97
16	4.11	1.00	5557	±5.04	5509	±6.53	5533	±4.12	0.87
17	4.11	1.49	5990	±4.74	5945	±9.01	5968	±5.08	0.76
18	4.02	2.00	7419	±3.91	7339	±9.75	7379	±5.23	1.08
19	1.89	0.50	4114	±3.41	4103	±4.49	4108	±2.82	0.26
20	1.89	0.50	4228	±3.32	4219	±4.37	4223	±2.74	0.21
21	1.89	0.50	4114	±3.41	4121	±4.47	4117	±2.81	0.15
22	1.87	0.50	4788	±2.89	4779	±3.88	4783	±2.42	0.19
23	1.88	0.50	4827	±2.86	4832	±3.83	4830	±2.39	0.10
24	1.88	0.50	4771	±2.90	4777	±3.87	4774	±2.42	0.13
25	1.87	0.50	5109	±2.69	5125	±3.63	5117	±2.26	0.32
26	1.88	0.50	5011	±2.74	5057	±3.68	5034	±2.30	0.91
27	1.88	0.50	4900	±2.81	4948	±3.75	4924	±2.35	0.96
28	1.90	0.50	4686	±3.09	4738	±3.91	4712	±2.49	1.11
29	2.08	1.00	4430	±3.51	4476	±8.03	4453	±4.40	1.04
30	2.10	1.00	4527	±3.73	4571	±7.87	4549	±4.37	0.96
31	2.08	1.00	4388	±3.56	4437	±8.10	4412	±4.44	1.11
32	1.98	1.00	4150	±3.48	4135	±8.68	4142	±4.67	0.37
33	1.99	1.00	4536	±3.15	4536	±7.92	4536	±4.26	0.00
34	1.99	1.00	4261	±3.46	4231	±8.48	4246	±4.57	0.72
35	1.99	1.00	6134	±2.36	6103	±5.92	6118	±3.18	0.52
36	1.98	1.00	5852	±2.48	5803	±6.22	5828	±3.34	0.84
37	2.04	1.01	5997	±2.48	6062	±6.02	6029	±3.27	1.07
38	2.03	1.01	6063	±2.45	6145	±5.94	6104	±3.23	1.35
39	2.04	1.01	6027	±2.42	6054	±6.02	6041	±3.25	0.45
40	2.05	1.01	5973	±2.50	6007	±6.08	5990	±3.29	0.57
41	2.05	1.01	5860	±2.50	5957	±6.12	5909	±3.33	1.62
42	1.97	1.00	6717	±2.18	6694	±5.41	6705	±2.91	0.34
43	2.90	0.50	3758	±5.30	3738	±4.91	3748	±3.61	0.52
44	2.89	0.50	3646	±5.43	3594	±5.09	3620	±3.72	1.45
45	2.85	0.50	4649	±4.25	4746	±3.91	4698	±2.88	2.05
46	2.82	0.50	4800	±4.18	4815	±3.86	4808	±2.84	0.30
47	2.87	0.50	5217	±3.74	5148	±3.62	5182	±2.60	1.34
48	2.88	0.50	5033	±3.88	4983	±3.72	5008	±2.69	1.01
49	2.82	0.50	5698	±3.37	5742	±3.27	5720	±2.35	0.77
50	2.82	0.50	5850	±3.28	5815	±3.23	5833	±2.30	0.60
...	...	...	...	...	...	...	...	...	...
64	2.88	1.52	6081	±3.26	6111	±8.90	6096	±4.75	0.50

* $\dot{Q}_{exp} = 0.5(\dot{Q}_a + \dot{Q}_r)$

Table 5.3: Calculated experimental results

5.3.2 Energy balance checks

The cooling capacities determined independently from the measurements on the air- and refrigerant-side are checked for agreement, in order to fulfil the energy conservation law. The resulting capacities obtained on both sides of the heat exchanger are expected to agree within their uncertainty intervals.
A comparative plot of the experimental cooling capacities with uncertainty intervals is presented in Figure 5.4. Good agreement for the independent measurements is observed. As can be seen, the uncertainty intervals of the experimental cooling capacities are highly dependent on the test conditions. In the majority of cases the uncertainty of the cooling capacity obtained refrigerant-side is higher than the obtained air-side. This is due to the very small refrigerant temperature lifts present in some cases. Although the measurement of the refrigerant temperature has smaller uncertainty than the air temperature measurement, the cooling capacity, based on the temperature difference measurement, presents larger uncertainty.

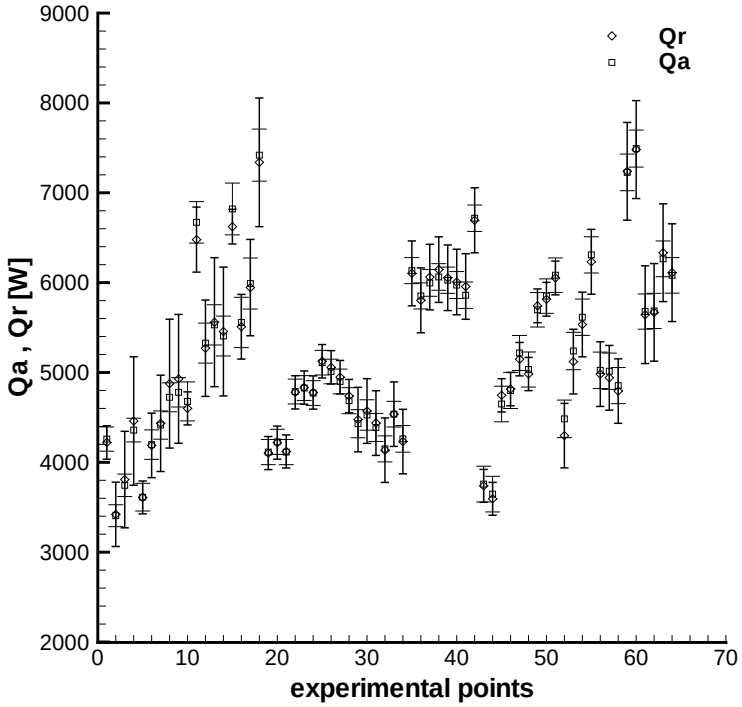

Figure 5.4: Agreement of refrigerant- and air-side cooling capacities

5.3.3 Validation methodology for the heat exchanger

An experimental validation methodology for the compact heat exchanger model is presented, based on systematic comparisons of numerical with experimental results in a working range representative for engineering applications. The comparisons are focused on checking the capabilities of the numerical model to predict the thermal and fluid-dynamic behaviour of the heat exchanger in four aspects: cooling capacity, air pressure loss, refrigerant pressure loss, and latent cooling load prediction. The numerical to experimental comparisons and their statistical analysis are carried out automatically by means of a specially developed for this purpose Perl program, described in more detail in section 4.7.

The methodology can be used for different purposes, as to study the implication of the model complexity level over the accuracy of the results, empirical correlations evaluation and comparisons, experimental validation for different working ranges, etc.

The numerically calculated and the experimentally determined cooling capacities with their experimental uncertainties are presented together with the numerical to experimental difference (δ) calculated from equation (5.3) in Table 5.4 (whole data not presented here, but included in statistical analysis). As can be seen, for the majority of the studied cases the numerical-experimental differences for the cooling capacity

Case	$\dot{Q}_{num}$ [W]	$\dot{Q}_{exp}$ [W]	U_{exp} [%]	δ [%]	Case	$\dot{Q}_{num}$ [W]	$\dot{Q}_{exp}$ [W]	U_{exp} [%]	δ [%]
1	4296	4240	±2.71	1.34	27	4947	4924	±2.35	0.47
2	3513	3414	±5.54	2.92	28	4756	4712	±2.49	0.93
3	3866	3776	±7.30	2.37	29	4574	4453	±4.40	2.71
4	4522	4410	±8.25	2.53	30	4723	4549	±4.37	3.83
5	3691	3611	±3.31	2.23	31	4548	4412	±4.44	3.07
6	4376	4193	±4.70	4.37	32	4137	4142	±4.67	-0.14
7	4630	4425	±6.31	4.65	33	4541	4536	±4.26	0.10
8	4974	4800	±7.66	3.62	34	4244	4246	±4.57	-0.04
9	5025	4854	±7.57	3.53	35	6028	6118	±3.18	-1.47
10	4735	4639	±3.07	2.07	36	5774	5828	±3.34	-0.92
11	6820	6575	±3.26	3.73	37	6066	6029	±3.27	0.62
12	5595	5299	±5.48	5.59	38	6208	6104	±3.23	1.71
13	5809	5545	±6.78	4.76	39	6147	6041	±3.25	1.76
14	5677	5431	±6.91	4.52	40	6010	5990	±3.29	0.34
15	6809	6722	±2.58	1.29	41	6039	5909	±3.33	2.21
16	5844	5533	±4.12	5.64	42	6720	6705	±2.91	0.21
17	6335	5968	±5.08	6.15	43	3677	3748	±3.61	-1.89
18	7712	7379	±5.23	4.51	44	3550	3620	±3.72	-1.93
19	4106	4108	±2.82	-0.06	45	4621	4698	±2.88	-1.64
20	4232	4223	±2.74	0.22	46	4665	4808	±2.84	-2.97
21	4136	4117	±2.81	0.46	47	5167	5182	±2.60	-0.29
22	4799	4783	±2.42	0.33	48	5002	5008	±2.69	-0.14
23	4819	4830	±2.39	-0.23	49	5731	5720	±2.35	0.19
24	4788	4774	±2.42	0.30	50	5812	5833	±2.30	-0.36
25	5136	5117	±2.26	0.37	...	...	...	...	...
26	5062	5034	±2.30	0.55	64	6287	6096	±4.75	3.14

Table 5.4: Cooling capacity: Experimental to numerical comparison

are within the experimental uncertainty interval. For the compared cases statistical analyses have been executed in order to determine the average numerical to experimental differences ($\bar{\delta}$) and their dispersions (S). The analyses have been performed for the data set as a whole, and for groups of cases divided according ranges of air velocity, refrigerant velocity, and dry and wet cases. The analyses for groups are intended to reveal if the differences are larger in some specific working conditions. The results from the statistical analyses of the cooling capacity numerical-experimental differences are presented in Table 5.5 to Table 5.8. It can be seen that as an average the numerical model over-predicts the experimental capacity 1.56%, but this falls within the average uncertainty interval of the experimental results, which is 3.97%. The maximum difference between the numerical and the experimental results is 6.15%. From the analyses for groups cannot be observed larger differences for some specific working range, being these within the uncertainty interval of the experimental results.

Points	$\bar{U}_{exp}$ [%]	$\bar{\delta}$ [%]	S_δ [%]	$\lvert\bar{\delta}\rvert$ [%]	$S_{\lvert\delta\rvert}$ [%]	Max [%]	Min [%]
64	±3.97	1.56	1.98	1.96	1.58	6.15	-2.97

Table 5.5: Cooling capacity: Analysis for the whole data set

Zone	Points	$\bar{U}_{exp}$ [%]	$\bar{\delta}$ [%]	S_δ [%]	$\lvert\bar{\delta}\rvert$ [%]	$S_{\lvert\delta\rvert}$ [%]	Max [%]	Min [%]
$V_a \approx 1.5m/s$	4	±5.95	2.29	0.59	2.29	0.59	2.92	1.34
$V_a \approx 2.0m/s$	29	±3.69	1.23	1.61	1.43	1.44	4.65	-1.47
$V_a \approx 3.0m/s$	27	±3.94	1.39	2.12	2.13	1.38	5.59	-2.97
$V_a \approx 4.0m/s$	4	±4.25	4.40	1.89	4.40	1.89	6.15	1.29

Table 5.6: Cooling capacity: Analysis for ranges of air velocity

Zone	Points	$\bar{U}_{exp}$ [%]	$\bar{\delta}$ [%]	S_δ [%]	$\lvert\bar{\delta}\rvert$ [%]	$S_{\lvert\delta\rvert}$ [%]	Max [%]	Min [%]
$V_r \approx 0.5m/s$	23	±2.69	0.02	1.22	0.91	0.81	2.23	-2.97
$V_r \approx 1.0m/s$	25	±3.94	1.73	1.68	1.93	1.44	5.64	-1.47
$V_r \approx 1.5m/s$	10	±5.16	3.28	1.56	3.28	1.56	6.15	1.18
$V_r \approx 2.0m/s$	6	±7.07	3.91	0.77	3.91	0.77	4.76	2.53

Table 5.7: Cooling capacity: Analysis for ranges of refrigerant velocity

Zone	Points	$\bar{U}_{exp}$ [%]	$\bar{\delta}$ [%]	S_δ [%]	$\lvert\bar{\delta}\rvert$ [%]	$S_{\lvert\delta\rvert}$ [%]	Max [%]	Min [%]
Dry tests	18	±5.33	3.66	1.43	3.66	1.43	6.15	1.29
Wet tests	46	±3.44	0.74	1.50	1.30	1.05	3.83	-2.97

Table 5.8: Cooling capacity: Analysis for dry and wet cases

The experimental validation of the model with respect to the air pressure loss calculation is carried out through numerical-experimental comparisons and their statistical analysis. In Table 5.9 are presented the numerically calculated air pressure loss through the heat exchanger, the experimental value, its uncertainty interval, and the numerical-experimental difference (δ). Statistical analyses of the results are presented in Table 5.10 to Table 5.12. As can be observed from the results, the predicted air pressure loss from the model differs in absolute terms as an average 21.77% from the experimental results, with maximum difference of 61.52%. The differences present wide dispersion, varying from positive to negative values. The average difference ($\bar{\delta}$) for the whole data set is near zero, meaning that over-estimation and under-estimation of the air pressure loss from the model are equally probable. The analysis for ranges of air velocity shows that numerical-experimental differences are larger for lower and higher velocities (1.5 and 4 m/s), and over-prediction of the experimental values is present. In the moderate air velocity range (2 and 3 m/s) the differences are slightly lower than the average for the whole data set, and range from over-prediction to under-prediction of the experimental result. The analysis for dry and wet cases shows clearly that in dry test conditions the numerical model calculates higher values than the experimental air pressure losses, 38.62% as an average, and that under-predicts it in wet cases as an average of 15.17%.

Case	P_{apl}^{num} $[Pa]$	P_{apl}^{exp} $[Pa]$	U_{apl} [%]	δ [%]	Case	P_{apl}^{num} $[Pa]$	P_{apl}^{exp} $[Pa]$	U_{apl} [%]	δ [%]
1	41.1	25.4	±10.02	61.52	27	53.8	64.4	±3.96	-16.48
2	36.4	25.5	±9.99	42.68	28	54.5	63.7	±4.00	-14.53
3	35.2	26.8	±9.51	31.30	29	63.2	80.8	±3.15	-21.85
4	36.8	24.2	±10.53	51.96	30	64.2	80.5	±3.17	-20.19
5	59.6	44.8	±5.70	33.23	31	63.6	80.6	±3.16	-21.04
6	59.5	44.5	±5.74	33.78	32	59.3	63.9	±3.99	-7.20
7	58.1	45.1	±5.65	28.86	33	59.5	62.8	±4.06	-5.28
8	57.5	45.5	±5.60	26.16	34	59.4	63.5	±4.02	-6.36
9	56.6	46.4	±5.50	22.05	35	58.6	63.5	±4.02	-7.71
10	124.4	90.2	±2.83	37.96	36	58.6	63.4	±4.02	-7.65
11	115.9	74.4	±3.43	55.77	37	61.4	81.6	±3.13	-24.72
12	122.6	92.9	±2.74	31.94	38	61.1	81.1	±3.15	-24.67
13	120.1	94.9	±2.69	26.55	39	61.5	81.7	±3.12	-24.65
14	119.7	95.3	±2.67	25.58	40	61.9	81.3	±3.14	-23.87
15	189.3	121.6	±2.10	55.68	41	61.8	80.3	±3.17	-23.04
16	201.5	145.0	±1.76	38.95	42	57.9	63.7	±4.00	-9.03
17	201.2	148.9	±1.71	35.14	43	113.1	122.7	±2.08	-7.82
18	192.3	123.2	±2.07	56.08	44	112.3	123.2	±2.07	-8.81
19	54.0	65.5	±3.89	-17.64	45	109.1	124.4	±2.05	-12.30
20	54.1	65.5	±3.89	-17.44	46	107.3	126.4	±2.02	-15.11
21	54.1	65.4	±3.90	-17.23	47	109.1	133.7	±1.91	-18.39
22	53.2	65.9	±3.87	-19.22	48	109.8	133.3	±1.91	-17.63
23	53.4	65.9	±3.87	-18.92	49	105.8	135.9	±1.88	-22.15
24	53.3	65.9	±3.87	-19.23	50	105.9	135.8	±1.88	-21.98
25	53.2	65.2	±3.91	-18.47	...	...	...	...	...
26	53.4	65.1	±3.92	-18.03	64	110.9	135.3	±1.88	-18.03

Table 5.9: Air pressure loss: Numerical to experimental comparison

Points	$\bar{U}_{apl}$ [%]	$\bar{\delta}$ [%]	S_δ [%]	$\lvert\bar{\delta}\rvert$ [%]	$S_{\lvert\delta\rvert}$ [%]	Max [%]	Min [%]
64	±3.47	-0.04	25.67	21.77	13.60	61.52	-24.72

Table 5.10: Air pressure loss: Analysis for the whole data set

Zone	Points	$\bar{U}_{apl}$ [%]	$\bar{\delta}$ [%]	S_δ [%]	$\lvert\bar{\delta}\rvert$ [%]	$S_{\lvert\delta\rvert}$ [%]	Max [%]	Min [%]
$V_a \approx 1.5m/s$	4	±10.01	56.52	14.88	56.52	14.88	61.52	31.30
$V_a \approx 2.0m/s$	29	±4.02	-9.50	18.25	19.44	7.48	33.78	-24.72
$V_a \approx 3.0m/s$	27	±2.13	-4.28	20.55	17.46	11.65	55.77	-22.15
$V_a \approx 4.0m/s$	4	±1.91	46.46	9.52	46.46	9.52	56.08	35.14

Table 5.11: Air pressure loss: Analysis for ranges of air velocity

Zone	Points	$\bar{U}_{apl}$ [%]	$\bar{\delta}$ [%]	S_δ [%]	$\lvert\bar{\delta}\rvert$ [%]	$S_{\lvert\delta\rvert}$ [%]	Max [%]	Min [%]
Dry tests	18	±5.01	38.62	12.05	38.62	12.05	61.52	22.05
Wet tests	46	±2.86	-15.17	6.77	15.17	6.76	0.09	-24.72

Table 5.12: Air pressure loss: Analysis for dry and wet cases

The refrigerant pressure loss comparisons are presented in Table 5.13. The statistical analyses for the whole data set and for ranges of refrigerant velocity are given respectively in Tables 5.14 and 5.15. The comparisons of the numerical and experimental results show that the numerical model systematically under-predicts the experimental refrigerant pressure loss. The average difference is 20.3% with standard deviation of 1.77%. The average experimental uncertainty is 8.38% of the measured refrigerant pressure loss.

The analysis for ranges does not show any appreciable difference for the different ranges of refrigerant velocity. The numerically calculated pressure losses are between approximately 19 and 22% lower than the experimentally measured values for all of the studied groups.

The very consistent bias of the numerical results from the experimental values indicate that the numerical results can be improved by revision of some empiric parameters used in the simulations. One of the reasons may be the use in the simulations of rugosity lower than the present in the experiments. The rugosity is a parameter difficult to evaluate precisely, and the available empirical information presents wide range of dispersion of the given values. Another reason for such a differences with the experimental data may be due to the empirical data for the pressure loss in singularities, as elbows, sudden contractions and expansions, flow division and merging in the collectors. Different correlations for the friction factor should also be studied.

Case	P_{rpl}^{num} [Pa]	P_{rpl}^{exp} [Pa]	U_{rpl} [%]	δ [%]	Case	P_{rpl}^{num} [Pa]	P_{rpl}^{exp} [Pa]	U_{rpl} [%]	δ [%]
1	1777	2246	±16.70	-20.86	27	1765	2273	±16.50	-22.35
2	6297	7798	±4.81	-19.25	28	1742	2289	±16.38	-23.89
3	13083	16400	±2.29	-20.23	29	6298	7995	±4.69	-21.22
4	22050	27750	±1.35	-20.54	30	6298	7968	±4.71	-20.96
5	1745	2164	±17.33	-19.37	31	6303	7988	±4.69	-21.10
6	6289	7778	±4.82	-19.15	32	6296	7766	±4.83	-18.92
7	13009	16280	±2.30	-20.09	33	6290	7765	±4.83	-18.99
8	22144	27830	±1.35	-20.43	34	6292	7767	±4.83	-18.99
9	22114	27780	±1.35	-20.40	35	6280	7712	±4.86	-18.57
10	1739	2163	±17.34	-19.62	36	6280	7722	±4.86	-18.67
11	6269	7699	±4.87	-18.57	37	6391	8016	±4.68	-20.27
12	12962	16010	±2.34	-19.04	38	6386	7914	±4.74	-19.30
13	22146	27800	±1.35	-20.34	39	6382	7931	±4.73	-19.53
14	22130	27790	±1.35	-20.37	40	6396	8037	±4.67	-20.42
15	1827	2212	±16.95	-17.40	41	6392	7937	±4.72	-19.47
16	6264	7755	±4.84	-19.23	42	6251	7678	±4.88	-18.58
17	12921	15900	±2.36	-18.73	43	1756	2192	±17.11	-19.90
18	21938	27570	±1.36	-20.43	44	1754	2212	±16.95	-20.70
19	1752	2271	±16.51	-22.84	45	1769	2185	±17.16	-19.03
20	1752	2275	±16.48	-22.99	46	1771	2175	±17.24	-18.58
21	1752	2279	±16.45	-23.11	47	1738	2303	±16.28	-24.52
22	1742	2277	±16.47	-23.50	48	1733	2256	±16.62	-23.20
23	1740	2261	±16.59	-23.06	49	1757	2250	±16.67	-21.90
24	1740	2266	±16.55	-23.22	50	1727	2244	±16.71	-23.06
25	1737	2266	±16.55	-23.35	...	...	...	...	...
26	1732	2271	±16.51	-23.72	64	13277	16390	±2.29	-18.99

Table 5.13: Refrigerant pressure loss: Numerical to experimental comparison

Points	$\bar{U}_{rpl}$ [%]	$\bar{\delta}$ [%]	S_δ [%]	$\lvert\bar{\delta}\rvert$ [%]	$S_{\lvert\delta\rvert}$ [%]	Max [%]	Min [%]
64	±8.38	-20.30	1.77	20.30	1.77	-17.40	-24.52

Table 5.14: Refrigerant pressure loss: Analysis for the whole data set

Zone	Points	$\bar{U}_{rpl}$ [%]	$\bar{\delta}$ [%]	S_δ [%]	$\lvert\bar{\delta}\rvert$ [%]	$S_{\lvert\delta\rvert}$ [%]	Max [%]	Min [%]
$V_r \approx 0.5m/s$	23	±16.73	-21.86	1.94	21.86	1.94	-17.40	-24.52
$V_r \approx 1.0m/s$	25	±4.80	-19.29	0.82	19.29	0.82	-18.57	-21.22
$V_r \approx 1.5m/s$	10	±2.30	-19.17	0.51	19.17	0.51	-18.73	-20.23
$V_r \approx 2.0m/s$	6	±1.35	-20.42	0.06	20.42	0.06	-20.34	-20.54

Table 5.15: Refrigerant pressure loss: Analysis for ranges of refrigerant velocity

The experimental validation for the latent cooling load prediction of the model is based on the comparisons of the condensed rate calculated numerically, and measured experimentally. The numerical and the experimental results, and their differences are presented in Table 5.16. A statistical analysis for the whole data set of wet cases is presented in Table 5.17. From the results can be observed that the absolute average numerical-experimental difference in the condensed rate is 3.42%, with numerical results ranging from under-prediction to over-prediction of the experimental results.

Case	$\dot{m}_{cond}^{num}$ $[\frac{kg}{h}]$	$\dot{m}_{cond}^{exp}$ $[\frac{kg}{h}]$	U_{cond} [%]	δ [%]
19	2.151	2.120	± 3.77	1.44
20	2.334	2.280	± 3.51	2.36
21	2.191	2.120	± 3.77	3.37
22	3.458	3.400	± 2.35	1.70
23	3.502	3.480	± 2.30	0.63
24	3.445	3.380	± 2.37	1.91
25	4.112	4.040	± 1.98	1.77
26	4.052	3.940	± 2.03	2.84
27	3.941	3.840	± 2.08	2.62
28	3.722	3.580	± 2.83	3.98
29	1.730	1.600	± 5.00	8.13
30	1.891	1.695	± 7.08	11.54
31	1.645	1.490	± 5.37	10.37
32	2.001	2.023	± 3.39	-1.06
33	2.406	2.427	± 2.25	-0.86
34	2.129	2.160	± 3.70	-1.43
35	4.525	4.731	± 1.45	-4.36
36	4.260	4.412	± 1.60	-3.44
37	4.816	4.860	± 1.65	-0.90
38	5.036	5.000	± 1.60	0.71
39	4.911	4.881	± 1.33	0.60
40	4.719	4.800	± 1.67	-1.69
41	4.726	4.629	± 1.48	2.11
42	5.836	5.876	± 1.41	-0.67
43	1.015	1.180	± 6.78	-13.97
44	0.909	1.090	± 7.34	-16.59
45	2.758	2.856	± 3.36	-3.44
46	2.802	3.029	± 3.77	-7.47
47	3.377	3.360	± 2.38	0.51
48	3.161	3.120	± 2.56	1.30
49	4.330	4.231	± 1.96	2.34
50	4.395	4.400	± 1.82	-0.11
...	...	...	...	...
64	4.570	4.460	± 1.79	2.47

Table 5.16: Condensed rate: Numerical to experimental comparison

Zone	Points	$\bar{U}_{cond}$ [%]	$\bar{\delta}$ [%]	S_δ [%]	$\lvert\bar{\delta}\rvert$ [%]	$S_{\lvert\delta\rvert}$ [%]	Max [%]	Min [%]
Wet tests	46	±2.78	0.65	4.88	3.42	3.54	11.54	-16.59

Table 5.17: Condensed rate: Analysis for wet cases

The results of the numerical to experimental comparisons are presented in graphical form for qualitative assessment in Figure 5.5. In the figure are presented the comparisons in the four aspects: cooling capacity, air and refrigerant pressure loss, and condensed rate. The experimental results are plotted in the abscissa, and the numerical in the ordinate. A range of deviation of the numerical results from the experimental is shown with dotted lines.

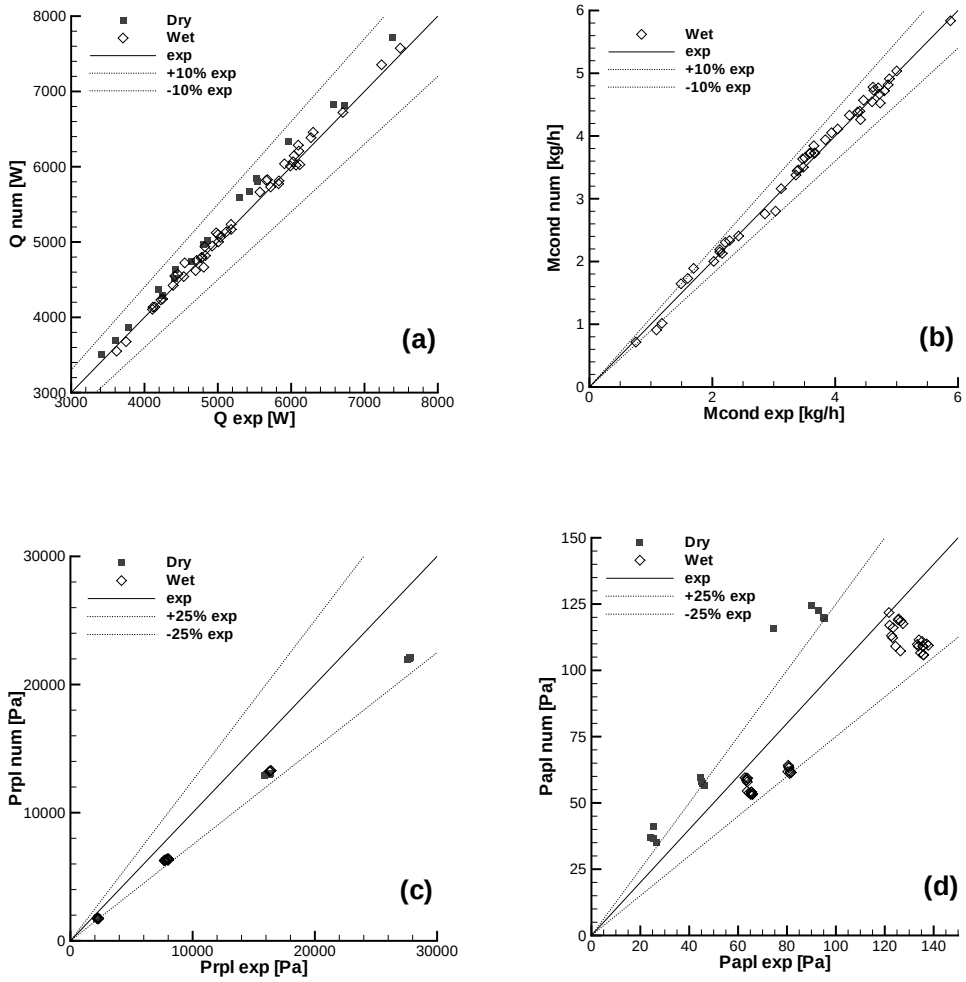

Figure 5.5: Graphical numerical to experimental comparisons: (a) heat transfer capacity; (b) condensed flow; (c) refrigerant pressure loss; (d) air pressure loss.

5.4 Galvanized steel heat exchanger

The heat exchanger prototype is made of carbon steel tubes and fins, galvanized externally with immersion in hot bath, thus assuring good thermal contact between tubes and fins. Galvanized heat exchangers have very good corrosion resistance and can be used in aggressive environments. The prototype has been constructed with a single refrigerant circuit, passing through all of the tubes. This arrangement assures higher refrigerant temperature lift through the heat exchanger, which leads to higher accuracy in the temperature difference measurement, resulting in lower uncertainty in the cooling capacity determined refrigerant-side. The single circuit arrangement is also favourable to the refrigerant pressure loss measurement and validation, because local pressure losses in flow expansions and contractions are avoided, guaranteeing more forward conditions for comparison of the experimental and numerical results.

Model	Prototype 2
Tubes' arrangement	Staggered
Number of tubes in depth (X)	4
Number of tubes in height (Y)	6
Number of circuits	1
Longitude of fins in X[mm]	225.14
Longitude of fins in Y[mm]	392.58
Longitude of the heat exchanger in Z[mm]	510
Tube distance in X (P_l)[mm]	56.66
Tube distance in Y (P_t)[mm]	65.43
Material of fins	Galvanized steel
Fin pitch (s)[mm]	6
Fin thickness [mm]	0.25
Type of fin	Plane
Material of tube	Galvanized steel
Exterior diameter of tube [mm]	22
Tube thickness [mm]	1.32

Table 5.18: Prototype definition

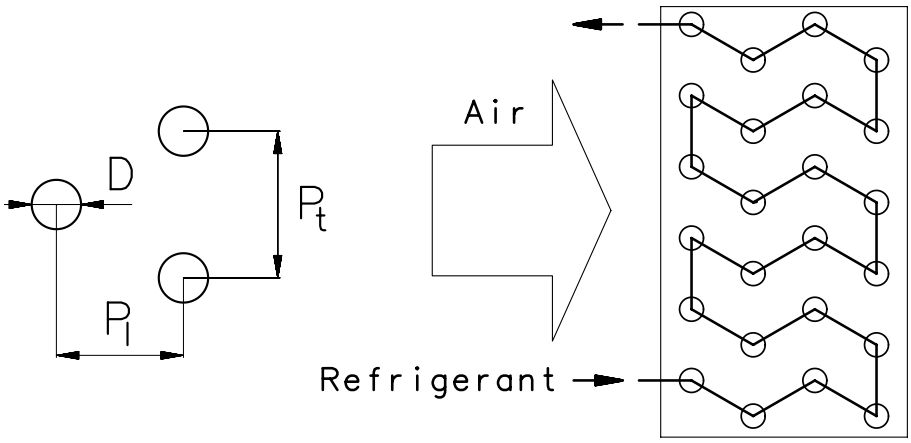

Figure 5.6: Tubes and refrigerant circuit arrangement

The arrangement of the tubes and the refrigerant circuit of the galvanized steel heat exchanger prototype is presented in Figure 5.6. The constructive drawing with dimensions of the prototype is shown in Figure 5.7.

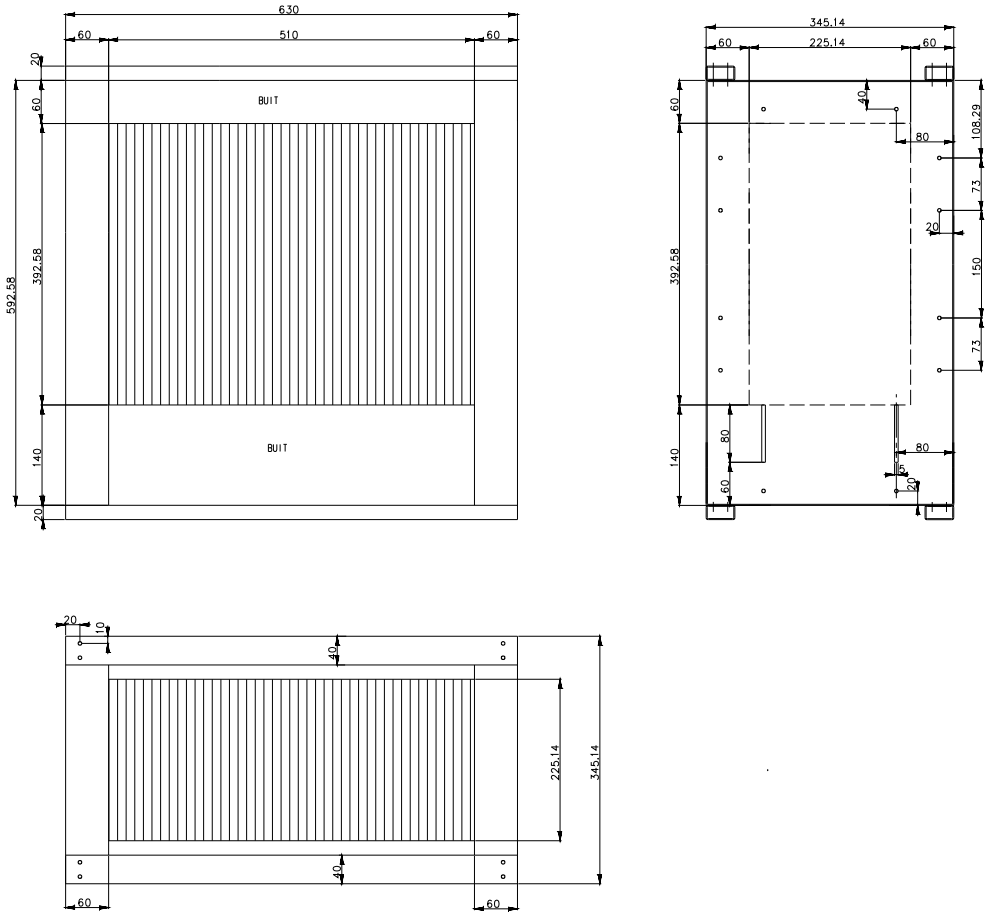

Figure 5.7: Construction and dimensions of the galvanized steel prototype

5.4.1 Experimental results

The experimental tests with the galvanized steel air-cooling heat exchanger prototype have been performed under steady state conditions. The conditions for the tests range from 0.51 to 7.29 m/s for the air velocity, 0.5 to 2.0 m/s for the refrigerant velocity, with inlet relative humidities from 35 to 85 %. The experimental data comprises 99 experimental cases, from which 28 are dry cases, and the rest are wet cases. Pure water has been used as a refrigerant. The temperature of the water at the inlet has been maintained in approximately 7^oC and the temperature of the air at the inlet ranges approximately from 20 to 32^oC.

The cooling capacity of the tested heat exchanger can be determined from the measurements independently on both air- and refrigerant-side. On the air-side the air mass flow-rate, the inlet and outlet temperatures and relative humidities are measured. For the wet experimental cases the condensed water vapour flux is measured in order to determine the latent cooling load over the heat exchanger. The relative humidity is measured with capacitance type sensors. Due to the decrease of the accuracy of these type of sensors in near saturation conditions ($\varphi > 90\%$), the relative humidity at the outlet has been calculated from the relative humidity at the inlet, the condensed flux and the air temperatures at the inlet and outlet using psychrometrics relations. The air pressure loss through the heat exchanger is measured with differential pressure transducer, using equalizing piezometric ring to average the pressure from four pressure taps in the walls of the duct, before and after the heat exchanger (see section 3.5.1).

The refrigerant flow-rate and the inlet and outlet refrigerant temperatures are measured on the refrigerant side. The refrigerant pressure loss through the heat exchanger is measured with differential pressure transducer. The average values of the experimentally measured variables are presented in Table 5.19.

The measured variables have been used to calculate the air and refrigerant velocities and the air- and refrigerant-side cooling capacities. The cooling capacities have been calculated using the formulation presented in sections 4.4.1 and 4.4.2. Their uncertainty intervals have been determined from the formulation presented in section 4.5. The stated as experimental cooling capacity ($\dot{Q}_{exp}$) is obtained as an arithmetic mean of the cooling capacities determined air- and refrigerant-side, with uncertainty calculated from equation 5.2. The difference between the cooling capacities determined both sides, relative to the experimental cooling capacity is also calculated. The calculated variables and results are presented in Table 5.20.

From the results can be seen that the experimental uncertainty, as a whole, is larger in the cooling capacity determined air-side, except for some cases. Higher uncertainties are estimated in cases where small temperature differences in the fluids between inlet and outlet are present, associated with higher velocities of the fluids, or small heat transfer capacities measured.

Case	$\dot{m}_a$ $[\frac{kg}{s}]$	T_{ai} $[C]$	T_{ao} $[C]$	φ_i [%]	$\varphi_o{}^*$ [%]	P_{apl}^{exp} $[Pa]$	$\dot{m}_{cond}$ $[\frac{kg}{h}]$	$\dot{m}_r$ $[\frac{kg}{h}]$	T_{ri} $[C]$	T_{ro} $[C]$	P_{rpl}^{exp} $[Pa]$
1	0.1218	25.20	12.28	36.75	82.49	5.8	0.000	1062	7.05	8.35	23850
2	0.1188	25.28	12.06	35.86	82.05	6.1	0.000	1062	7.05	8.32	23970
3	0.1188	25.23	11.82	35.46	82.19	6.0	0.000	1592	7.05	7.93	49330
4	0.2409	25.21	15.87	41.43	73.72	11.8	0.000	528	6.92	10.60	6934
5	0.2370	25.25	15.14	38.40	71.75	10.7	0.000	1060	7.03	8.99	23710
6	0.2364	25.39	14.82	37.50	72.16	10.2	0.000	1600	6.96	8.32	49420
7	0.2372	25.39	14.77	37.20	71.81	10.4	0.000	2112	7.13	8.18	82240
8	0.3285	25.16	17.22	43.21	70.36	16.1	0.000	528	6.96	11.19	6903
9	0.4729	25.08	18.65	44.11	65.31	26.7	0.000	526	7.01	11.93	6839
10	0.4726	25.12	17.84	40.79	63.68	25.0	0.000	1066	7.01	9.76	23870
11	0.4766	25.14	17.89	40.29	62.83	26.5	0.000	1058	7.02	9.80	23520
12	0.4769	25.18	17.53	38.91	62.16	26.2	0.000	1597	6.94	8.89	49190
13	0.4746	25.17	17.42	38.74	62.30	26.3	0.000	2107	7.12	8.63	81840
14	0.7088	25.05	20.12	45.89	61.90	49.3	0.000	526	7.03	12.76	6789
15	0.7117	25.12	19.34	41.21	58.55	49.0	0.000	1066	7.00	10.30	23780
16	0.7074	25.12	19.36	41.95	59.52	49.9	0.000	1056	6.99	10.30	23430
17	0.7097	25.15	19.04	39.14	56.77	49.8	0.000	1603	6.97	9.28	49430
18	0.7170	25.15	18.96	39.52	57.60	51.8	0.000	2115	7.11	8.94	82270
19	0.9552	25.07	20.95	48.21	61.83	75.8	0.000	525	7.04	13.38	6731
20	0.9482	25.12	20.23	43.59	58.62	77.2	0.000	1056	6.99	10.70	23390
21	0.9495	25.11	19.87	39.98	54.93	80.2	0.000	1602	6.94	9.54	49300
22	0.9494	25.13	19.77	40.25	55.73	78.5	0.000	2114	7.09	9.13	82170
23	1.1850	25.15	20.86	45.47	58.86	113.2	0.000	1054	6.99	11.08	23280
24	1.1920	25.13	20.59	41.29	54.30	120.0	0.000	1592	6.92	9.79	48660
25	1.4280	25.07	21.22	48.82	61.53	157.7	0.000	1053	6.98	11.40	23200
26	1.4110	25.12	21.09	42.31	53.92	164.8	0.000	1590	7.01	10.08	48490
27	1.6500	25.17	21.81	40.31	49.26	197.5	0.000	1057	7.04	11.54	23500
28	1.6800	25.12	21.50	43.24	53.70	222.3	0.000	1590	6.99	10.27	48460
29	0.1241	25.16	13.62	65.08	99.62	7.1	1.520	1063	7.01	9.04	24010
30	0.1232	25.19	14.33	74.91	99.96	7.0	2.170	1063	7.00	9.31	23920
31	0.1228	25.07	15.05	85.22	99.95	6.9	2.840	1062	7.00	9.59	23920
32	0.2377	25.02	16.12	64.98	94.72	13.5	1.800	1071	6.97	9.69	24230
33	0.2383	25.11	17.02	74.92	98.59	13.3	2.650	1060	6.93	10.08	23770
34	0.2374	25.14	17.97	85.18	98.56	13.2	3.834	1061	7.00	10.51	23690
35	0.4754	25.04	17.71	54.85	83.44	31.0	0.561	1071	6.96	10.06	24130
36	0.4711	25.01	18.01	60.22	87.59	31.6	1.100	1071	7.10	10.39	24160
37	0.4592	25.07	18.32	65.06	90.38	29.6	1.760	1057	7.06	10.54	23570
38	0.4666	25.00	18.71	70.17	94.05	32.4	2.110	1069	6.95	10.70	24060
39	0.4513	25.03	19.14	75.58	94.80	29.5	3.120	1057	7.01	10.94	23500
40	0.4564	24.95	19.37	79.96	96.40	33.6	3.840	1067	6.98	11.20	23860
41	0.4507	25.06	20.15	85.70	96.85	28.6	4.600	1057	7.08	11.44	23480
42	0.4780	25.39	17.87	54.99	83.08	28.4	0.900	1599	7.00	9.30	48900
43	0.4776	25.40	17.93	55.04	82.92	28.4	0.900	1600	6.99	9.29	48990
44	0.4759	25.41	17.89	54.99	83.05	28.4	0.900	1597	7.00	9.30	48780
45	0.4759	25.44	17.92	55.06	83.07	28.4	0.929	1597	7.01	9.31	48860
46	0.7197	25.03	20.15	65.28	85.33	60.8	0.965	527	7.02	13.55	6749
47	0.6933	25.02	20.75	74.83	91.97	62.7	1.960	526	7.09	14.30	6695
48	0.6853	25.04	21.68	86.04	96.73	64.4	3.590	524	7.07	15.21	6621
49	0.7305	25.00	19.23	55.58	78.35	58.0	0.220	1068	7.04	10.67	24060
50	0.7248	24.98	19.34	59.87	82.11	59.7	0.856	1069	7.03	10.85	23960
...	...	...	...	...	...	...	...	...	...	...	...
99	1.6790	25.04	22.25	85.18	95.66	224.4	5.130	1050	7.02	13.45	23000
*	φ_o is calculated from the other results										

Table 5.19: Measured experimental results

Case	V_a	V_r	$\dot{Q}_a$	U_a	$\dot{Q}_r$	U_r	$\dot{Q}^*_{exp}$	U_{exp}	$100\frac{\lvert\dot{Q}_a-\dot{Q}_r\rvert}{\dot{Q}_{exp}}$
	$[m/s]$	$[m/s]$	$[W]$	[%]	$[W]$	[%]	$[W]$	[%]	[%]
1	0.52	1.00	1592	±4.44	1611	±8.75	1602	±4.92	1.18
2	0.51	1.00	1589	±4.93	1573	±8.96	1581	±5.10	1.00
3	0.51	1.50	1612	±4.56	1620	±13.00	1616	±6.90	0.49
4	1.04	0.50	2279	±5.27	2264	±3.23	2271	±3.10	0.64
5	1.02	1.00	2424	±4.89	2425	±5.85	2424	±3.81	0.03
6	1.02	1.51	2530	±4.82	2540	±8.37	2535	±4.83	0.40
7	1.03	1.99	2550	±4.86	2584	±10.82	2567	±5.96	1.33
8	1.42	0.50	2644	±5.80	2603	±2.85	2623	±3.25	1.57
9	2.04	0.50	3080	±7.05	3017	±2.51	3049	±3.77	2.10
10	2.05	1.00	3481	±6.27	3414	±4.24	3447	±3.80	1.98
11	2.06	1.00	3503	±6.26	3428	±4.19	3465	±3.78	2.21
12	2.06	1.50	3691	±5.98	3631	±5.88	3661	±4.19	1.64
13	2.05	1.98	3723	±5.97	3696	±7.58	3709	±4.82	0.75
14	3.06	0.49	3546	±9.00	3512	±2.21	3529	±4.65	0.99
15	3.08	1.00	4162	±7.70	4096	±3.57	4129	±4.27	1.62
16	3.05	0.99	4121	±7.74	4074	±3.56	4098	±4.28	1.15
17	3.07	1.51	4388	±7.26	4313	±5.00	4351	±4.42	1.72
18	3.10	1.99	4491	±7.24	4496	±6.28	4493	±4.79	0.10
19	4.13	0.49	3992	±10.56	3878	±2.05	3935	±5.45	2.93
20	4.09	0.99	4702	±8.96	4571	±3.21	4637	±4.81	2.85
21	4.11	1.51	5037	±8.38	4846	±4.47	4942	±4.80	3.93
22	4.10	1.99	5157	±8.28	5026	±5.64	5091	±5.03	2.61
23	5.11	0.99	5142	±10.19	5018	±2.94	5080	±5.36	2.47
24	5.17	1.50	5480	±9.60	5337	±4.06	5409	±5.26	2.67
25	6.16	0.99	5577	±11.24	5423	±2.75	5500	±5.86	2.84
26	6.11	1.50	5770	±10.73	5696	±3.81	5733	±5.72	1.30
27	7.13	1.00	5609	±12.81	5547	±2.70	5578	±6.58	1.11
28	7.28	1.50	6169	±11.91	6085	±3.59	6127	±6.25	1.38
29	0.54	1.00	2511	±3.29	2516	±5.66	2514	±3.28	0.20
30	0.54	1.00	2868	±2.86	2863	±5.00	2866	±2.88	0.19
31	0.54	1.00	3226	±2.52	3199	±4.49	3212	±2.57	0.83
32	1.04	1.01	3398	±3.67	3395	±4.28	3397	±2.82	0.11
33	1.04	1.00	3802	±3.26	3885	±3.73	3843	±2.48	2.13
34	1.04	1.00	4393	±2.75	4335	±3.38	4364	±2.18	1.35
35	2.08	1.01	3926	±5.69	3865	±3.79	3896	±3.43	1.57
36	2.06	1.01	4114	±5.38	4101	±3.59	4107	±3.23	0.31
37	1.98	1.00	4370	±4.93	4283	±3.40	4326	±3.01	2.04
38	2.04	1.01	4448	±4.90	4674	±3.18	4561	±2.89	4.84
39	1.96	1.00	4870	±4.32	4838	±3.05	4854	±2.65	0.67
40	2.00	1.00	5255	±4.04	5244	±2.86	5249	±2.47	0.20
41	1.95	1.00	5443	±3.83	5371	±2.78	5407	±2.37	1.33
42	2.07	1.51	4273	±5.27	4280	±5.03	4276	±3.64	0.18
43	2.06	1.51	4248	±5.30	4290	±5.02	4269	±3.65	0.99
44	2.06	1.50	4255	±5.27	4280	±5.02	4268	±3.64	0.59
45	2.06	1.50	4279	±5.24	4290	±5.01	4285	±3.63	0.25
46	3.11	0.50	4242	±7.71	4010	±2.00	4126	±4.08	5.78
47	3.02	0.49	4371	±7.11	4415	±1.86	4393	±3.66	1.00
48	2.99	0.49	4821	±6.34	4966	±1.71	4894	±3.24	2.91
49	3.18	1.01	4427	±7.48	4515	±3.27	4471	±4.06	1.96
50	3.16	1.01	4745	±6.94	4753	±3.13	4749	±3.81	0.18
...	...	...	...	...	...	...	...	...	...
99	7.29	0.99	8317	±8.85	7870	±2.02	8093	±4.65	5.68

* $\dot{Q}_{exp} = 0.5(\dot{Q}_a + \dot{Q}_r)$

Table 5.20: Calculated experimental results

5.4.2 Energy balance checks

The fulfilling of the energy conservation law has been checked for all of the experimental points. The cooling capacities determined on both air- and refrigerant-side have been checked for agreement, plotted with their respective uncertainty intervals in Figure 5.8. The experimental results show very good agreement, with uncertainty intervals overlapping completely in all of the cases. This is a strong verification of the experimental results.
It can be observed that the uncertainty intervals of the cooling capacity refrigerant-side are smaller, which is due to the fact that the tested heat exchanger prototype has only one refrigerant circuit, leading to higher temperature lift in the refrigerant.

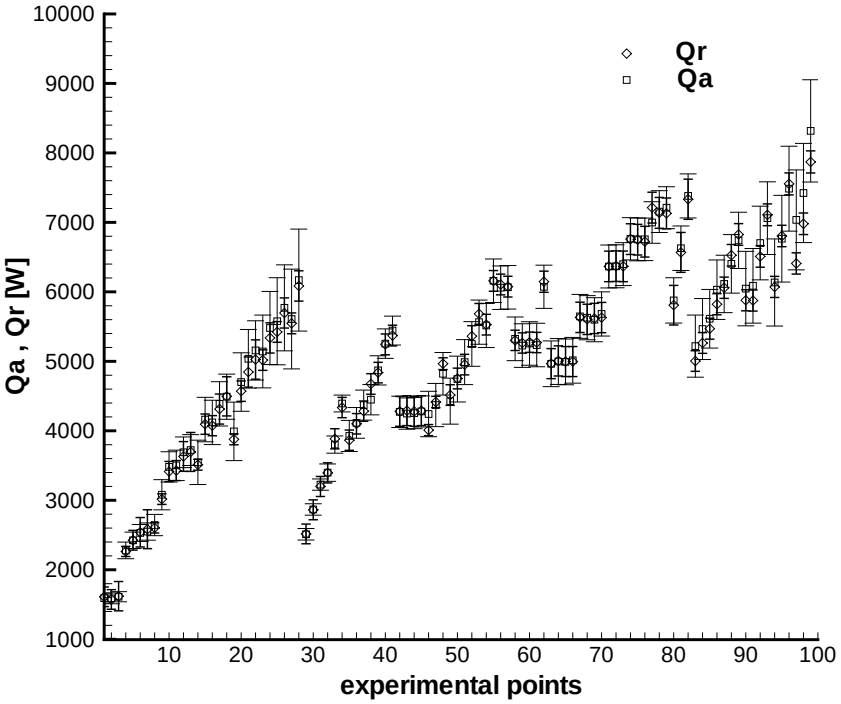

Figure 5.8: Agreement of refrigerant- and air-side cooling capacities

5.4.3 Validation methodology for the heat exchanger

The validation methodology for the simulation model, using experimental data for galvanized steel compact heat exchanger, is illustrated with systematic comparisons of the numerical and experimental results, and analysis of the observed differences. The same methodology can be applied for detailed validation studies concerning the use of different empirical correlations, numerical discretization, or level of complexity of the models.
The presented experimental results are based on the average values measured during the experiment, and thus are the most probable results for the experimental points, but the true results can lie anywhere within the corresponding uncertainty intervals. The experimental uncertainty is the resolution to which clear conclusions can be made when comparing experimental and numerical results, [1]. A care should be taken when concluding over the capabilities of some model to describe better the experimental results than other, or if some correlation is better than other, if both numerical results fall within the uncertainty interval of the experimental result. In such cases more accurate and extense experimental data will be needed, in order to make the right conclusions.
In Table 5.21 the numerical and experimental cooling capacities, the uncertainties

Case	$\dot{Q}_{num}$ [W]	$\dot{Q}_{exp}$ [W]	U_{exp} [%]	δ [%]	Case	$\dot{Q}_{num}$ [W]	$\dot{Q}_{exp}$ [W]	U_{exp} [%]	δ [%]
1	1515	1602	±4.92	-5.40	27	5611	5578	±6.58	0.60
2	1491	1581	±5.10	-5.66	28	6243	6127	±6.25	1.89
3	1519	1616	±6.90	-5.98	29	2418	2514	±3.28	-3.80
4	2159	2271	±3.10	-4.95	30	2767	2866	±2.88	-3.43
5	2342	2424	±3.81	-3.40	31	3093	3212	±2.57	-3.73
6	2451	2535	±4.83	-3.29	32	3273	3397	±2.82	-3.63
7	2473	2567	±5.96	-3.68	33	3800	3843	±2.48	-1.14
8	2520	2623	±3.25	-3.94	34	4305	4364	±2.18	-1.35
9	2943	3049	±3.77	-3.46	35	3658	3896	±3.43	-6.10
10	3386	3447	±3.80	-1.80	36	3858	4107	±3.23	-6.07
11	3394	3465	±3.78	-2.05	37	4142	4326	±3.01	-4.26
12	3597	3661	±4.19	-1.75	38	4521	4561	±2.89	-0.88
13	3642	3709	±4.82	-1.80	39	4801	4854	±2.65	-1.09
14	3447	3529	±4.65	-2.31	40	5107	5249	±2.47	-2.72
15	4082	4129	±4.27	-1.13	41	5464	5407	±2.37	1.05
16	4079	4098	±4.28	-0.44	42	4036	4276	±3.64	-5.62
17	4340	4351	±4.42	-0.25	43	4045	4269	±3.65	-5.24
18	4481	4493	±4.79	-0.27	44	4035	4268	±3.64	-5.46
19	3834	3935	±5.45	-2.56	45	4046	4285	±3.63	-5.58
20	4627	4637	±4.81	-0.22	46	3780	4126	±4.08	-8.37
21	4939	4942	±4.80	-0.06	47	4148	4393	±3.66	-5.58
22	5106	5091	±5.03	0.29	48	4778	4894	±3.24	-2.37
23	5073	5080	±5.36	-0.15	49	4344	4471	±4.06	-2.84
24	5460	5409	±5.26	0.94	50	4460	4749	±3.81	-6.09
25	5480	5500	±5.86	-0.37	...	...	...	...	...
26	5819	5733	±5.72	1.50	99	7733	8093	±4.65	-4.46

Table 5.21: Cooling capacity: Experimental to numerical comparison

of the experimental results, and the numerical to experimental differences are shown. The numerical cooling capacities are obtained from simulations, and the experimental capacities are obtained from the measured variables according to the formulation presented in section 4.4. The uncertainties are evaluated using the methodology described in section 4.5. The calculation of the experimental results and the comparisons have been carried out automatically with a program using as input the results from the simulations and the pre-processed experimental data.
The results from the statistical analyses of the numerical to experimental differences are presented in Tables 5.22 to 5.25. The differences have been analysed for the whole data set and for groups divided according to ranges of air velocity, refrigerant velocity, and dry and wet cases. In the tables, together with the average, the absolute average

Points	$\bar{U}_{exp}$ [%]	$\bar{\delta}$ [%]	S_δ [%]	$\lvert\bar{\delta}\rvert$ [%]	$S_{\lvert\delta\rvert}$ [%]	Max [%]	Min [%]
99	±3.85	-3.10	2.39	3.26	2.17	1.89	-8.47

Table 5.22: Cooling capacity: Analysis for the whole data set

Zone	Points	$\bar{U}_{exp}$ [%]	$\bar{\delta}$ [%]	S_δ [%]	$\lvert\bar{\delta}\rvert$ [%]	$S_{\lvert\delta\rvert}$ [%]	Max [%]	Min [%]
$V_a \approx 0.5 m/s$	6	±4.27	-4.67	1.03	4.67	1.03	-3.43	-5.98
$V_a \approx 1.0 m/s$	8	±3.55	-3.17	1.21	3.17	1.21	-1.14	-4.95
$V_a \approx 2.0 m/s$	16	±3.44	-3.30	2.15	3.43	1.93	1.05	-6.10
$V_a \approx 3.0 m/s$	42	±3.42	-2.71	2.06	2.79	1.95	1.04	-8.37
$V_a \approx 4.0 m/s$	11	±4.29	-3.53	2.94	3.58	2.88	0.29	-8.47
$V_a \approx 5.0 m/s$	6	±4.66	-3.43	2.95	3.74	2.54	0.94	-6.57
$V_a \approx 6.0 m/s$	5	±5.16	-1.98	2.62	2.59	2.02	1.50	-5.26
$V_a \approx 7.0 m/s$	5	±5.60	-3.51	4.08	4.50	2.95	1.89	-7.82

Table 5.23: Cooling capacity: Analysis for ranges of air velocity

Zone	Points	$\bar{U}_{exp}$ [%]	$\bar{\delta}$ [%]	S_δ [%]	$\lvert\bar{\delta}\rvert$ [%]	$S_{\lvert\delta\rvert}$ [%]	Max [%]	Min [%]
$V_r \approx 0.5 m/s$	8	±3.90	-4.19	1.94	4.19	1.94	-2.31	-8.37
$V_r \approx 1.0 m/s$	55	±3.79	-3.16	2.50	3.28	2.34	1.05	-8.47
$V_r \approx 1.5 m/s$	29	±3.85	-2.90	2.19	3.20	1.72	1.89	-5.98
$V_r \approx 2.0 m/s$	7	±4.35	-2.23	2.30	2.31	2.21	0.29	-6.67

Table 5.24: Cooling capacity: Analysis for ranges of refrigerant velocity

Zone	Points	$\bar{U}_{exp}$ [%]	$\bar{\delta}$ [%]	S_δ [%]	$\lvert\bar{\delta}\rvert$ [%]	$S_{\lvert\delta\rvert}$ [%]	Max [%]	Min [%]
Dry tests	28	±4.85	-1.78	2.17	2.15	1.80	1.89	-5.98
Wet tests	71	±3.46	-3.62	2.27	3.70	2.14	1.05	-8.47

Table 5.25: Cooling capacity: Analysis for dry and wet cases

differences and their standard deviations, the mean experimental uncertainty for the respective group, and the minimum and maximum values of the difference for the group, are presented.
The numerical to experimental comparisons of the air pressure loss, and the statistical analysis of the differences are used for the validation of the numerical model. The experimental study of the air pressure loss of the heat exchanger comprises wide range of air velocities from 0.51 m/s up to 7.29 m/s, in dry and wet experimental tests. The numerical and experimental results and their differences are presented in Table 5.26. The numerical-experimental differences are found to be larger in the small velocity range, but the experimental uncertainty in this range is also the greatest. The numerical model under-estimates the experimental results up to 55.82%, and over-estimates it up to 23.11% for the available data set. From the statistical analyses of the differences for ranges of air velocity and dry and wet cases, presented respectively in Table 5.28 and Table 5.29, can be seen that the numerical model calculates lower air pressure loss than the experimentally measured in the lower range of air velocity, predicts reasonably well the pressure loss in the middle velocity range (2 - 3 m/s) with average differences in the order of the experimental uncertainty, and over-predicts the air pressure loss in higher velocities, for the studied heat exchanger.

Case	P_{apl}^{num} [Pa]	P_{apl}^{exp} [Pa]	U_{apl} [%]	δ [%]	Case	P_{apl}^{num} [Pa]	P_{apl}^{exp} [Pa]	U_{apl} [%]	δ [%]
1	3.0	5.8	±43.64	-48.15	27	229.8	197.5	±1.29	16.37
2	2.9	6.1	±41.79	-52.21	28	236.7	222.3	±1.15	6.50
3	2.9	6.0	±42.31	-51.65	29	3.1	7.1	±35.89	-55.82
4	9.1	11.8	±21.61	-23.11	30	3.1	7.0	±36.40	-55.65
5	8.8	10.7	±23.74	-18.05	31	3.1	6.9	±36.71	-55.41
6	8.8	10.2	±24.88	-14.36	32	8.9	13.5	±18.83	-34.21
7	8.8	10.4	±24.59	-14.87	33	8.9	13.3	±19.20	-32.77
8	15.1	16.1	±15.81	-6.52	34	8.9	13.2	±19.30	-32.78
9	27.8	26.7	±9.54	4.15	35	28.2	31.0	±8.22	-9.24
10	27.8	25.0	±10.21	11.35	36	27.7	31.6	±8.07	-12.36
11	28.2	26.5	±9.62	6.38	37	26.3	29.6	±8.62	-10.95
12	28.2	26.2	±9.73	7.75	38	27.2	32.4	±7.88	-15.77
13	28.0	26.3	±9.69	6.46	39	25.6	29.5	±8.65	-13.13
14	55.7	49.3	±5.18	13.11	40	26.3	33.6	±7.59	-21.77
15	56.1	49.0	±5.21	14.59	41	25.5	28.6	±8.92	-10.78
16	55.4	49.9	±5.11	11.09	42	28.3	28.4	±8.97	-0.39
17	55.8	49.8	±5.12	11.94	43	28.3	28.4	±8.96	-0.57
18	56.7	51.8	±4.93	9.62	44	28.1	28.4	±8.96	-1.27
19	93.3	75.8	±3.36	23.08	45	28.1	28.4	±8.97	-1.23
20	92.0	77.2	±3.30	19.22	46	57.1	60.8	±4.19	-6.13
21	92.3	80.2	±3.18	15.14	47	53.8	62.7	±4.07	-14.18
22	92.2	78.5	±3.25	17.42	48	52.8	64.4	±3.96	-18.09
23	133.1	113.2	±2.25	17.59	49	58.8	58.0	±4.39	1.25
24	134.8	120.0	±2.12	12.31	50	58.0	59.7	±4.27	-2.89
25	180.9	157.7	±1.62	14.73	...	...	...	...	...
26	177.9	164.8	±1.55	7.97	99	235.6	224.4	±1.14	5.00

Table 5.26: Air pressure loss: Numerical to experimental comparison

Points	$\bar{U}_{apl}$ [%]	$\bar{\delta}$ [%]	S_δ [%]	$\lvert\bar{\delta}\rvert$ [%]	$S_{\lvert\delta\rvert}$ [%]	Max [%]	Min [%]
99	±8.06	-4.62	16.90	12.30	12.47	23.11	-55.82

Table 5.27: Air pressure loss: Analysis for the whole data set

Zone	Points	$\bar{U}_{apl}$ [%]	$\bar{\delta}$ [%]	S_δ [%]	$\lvert\bar{\delta}\rvert$ [%]	$S_{\lvert\delta\rvert}$ [%]	Max [%]	Min [%]
$V_a \approx 0.5 m/s$	6	±39.46	-53.04	3.36	55.98	4.23	-48.15	-55.82
$V_a \approx 1.0 m/s$	8	±21.00	-22.92	9.79	23.39	9.83	-6.52	-34.21
$V_a \approx 2.0 m/s$	16	±8.91	-3.84	9.44	8.35	5.85	11.35	-21.77
$V_a \approx 3.0 m/s$	42	±4.63	-0.60	9.13	7.69	4.95	23.11	-18.09
$V_a \approx 4.0 m/s$	11	±2.82	2.54	13.96	12.59	6.54	23.08	-17.41
$V_a \approx 5.0 m/s$	6	±1.97	4.66	8.59	8.45	4.92	17.59	-6.94
$V_a \approx 6.0 m/s$	5	±1.52	5.87	6.07	7.32	4.23	14.73	-3.61
$V_a \approx 7.0 m/s$	5	±1.20	8.02	4.40	8.02	4.40	16.37	4.06

Table 5.28: Air pressure loss: Analysis for ranges of air velocity

Zone	Points	$\bar{U}_{apl}$ [%]	$\bar{\delta}$ [%]	S_δ [%]	$\lvert\bar{\delta}\rvert$ [%]	$S_{\lvert\delta\rvert}$ [%]	Max [%]	Min [%]
Dry tests	28	±11.99	0.64	21.17	16.99	12.65	23.08	-52.21
Wet tests	71	±6.51	-6.69	14.36	10.46	11.90	23.11	-55.82

Table 5.29: Air pressure loss: Analysis for dry and wet cases

The experimental validation of the model for the calculation of the refrigerant pressure loss is done comparing the numerical results with the experimental, and analyzing the observed differences. The numerical and experimental results, experimental uncertainties and numerical to experimental differences are presented in Table 5.30. For space availability only part of the results are shown in this table, however the whole data set is included in the statistical analysis presented in Table 5.31 and Table 5.32. The numerical refrigerant pressure loss is found to be systematically lower than the measured experimentally as an average of 27.05% for the whole data set, consisting of 99 experimental points. The observed differences have very low standard deviation of 0.74%. The analysis for ranges of refrigerant velocity does not show some dependence of the differences from the refrigerant velocity for the studied range. Study with different correlations for the friction factor, different empirical local pressure loss coefficients should be performed, in order to search better agreement with the experimental results. The value of the relative rugosity, used in the numerical model as a geometry parameter must also be reconsidered for correctness.

Case	P_{rpl}^{num} [Pa]	P_{rpl}^{exp} [Pa]	U_{rpl} [%]	δ [%]	Case	P_{rpl}^{num} [Pa]	P_{rpl}^{exp} [Pa]	U_{rpl} [%]	δ [%]
1	17275	23850	±1.57	-27.57	27	16975	23500	±1.60	-27.76
2	17276	23970	±1.56	-27.93	28	35454	48460	±0.77	-26.84
3	35748	49330	±0.76	-27.53	29	17273	24010	±1.56	-28.06
4	5092	6934	±5.41	-26.56	30	17261	23920	±1.57	-27.84
5	17188	23710	±1.58	-27.51	31	17220	23920	±1.57	-28.01
6	36046	49420	±0.76	-27.06	32	17476	24230	±1.55	-27.87
7	59729	82240	±0.46	-27.37	33	17140	23770	±1.58	-27.89
8	5080	6903	±5.43	-26.42	34	17144	23690	±1.58	-27.63
9	5047	6839	±5.48	-26.20	35	17462	24130	±1.55	-27.63
10	17323	23870	±1.57	-27.43	36	17441	24160	±1.55	-27.81
11	17091	23520	±1.59	-27.34	37	17028	23570	±1.59	-27.76
12	35873	49190	±0.76	-27.07	38	17371	24060	±1.56	-27.80
13	59409	81840	±0.46	-27.41	39	17008	23500	±1.60	-27.63
14	5020	6789	±5.52	-26.06	40	17288	23860	±1.57	-27.55
15	17297	23780	±1.58	-27.26	41	16977	23480	±1.60	-27.70
16	17009	23430	±1.60	-27.40	42	35923	48900	±0.77	-26.54
17	36077	49430	±0.76	-27.01	43	35965	48990	±0.77	-26.59
18	59781	82270	±0.46	-27.34	44	35842	48780	±0.77	-26.52
19	5000	6731	±5.57	-25.71	45	35840	48860	±0.77	-26.65
20	16988	23390	±1.60	-27.37	46	5028	6749	±5.56	-25.50
21	36012	49300	±0.76	-26.95	47	4995	6695	±5.60	-25.39
22	59699	82170	±0.46	-27.35	48	4949	6621	±5.66	-25.25
23	16913	23280	±1.61	-27.35	49	17342	24060	±1.56	-27.92
24	35584	48660	±0.77	-26.87	50	17366	23960	±1.57	-27.52
25	16869	23200	±1.62	-27.29	...	...	...	...	...
26	35471	48490	±0.77	-26.85	99	16691	23000	±1.63	-27.43

Table 5.30: Refrigerant pressure loss: Numerical to experimental comparison

Points	$\bar{U}_{rpl}$ [%]	$\bar{\delta}$ [%]	S_δ [%]	$\lvert\bar{\delta}\rvert$ [%]	$S_{\lvert\delta\rvert}$ [%]	Max [%]	Min [%]
99	±1.59	-27.05	0.74	27.05	0.74	-25.25	-28.06

Table 5.31: Refrigerant pressure loss: Analysis for the whole data set

Zone	Points	$\bar{U}_{rpl}$ [%]	$\bar{\delta}$ [%]	S_δ [%]	$\lvert\bar{\delta}\rvert$ [%]	$S_{\lvert\delta\rvert}$ [%]	Max [%]	Min [%]
$V_r \approx 0.5m/s$	8	±5.53	-25.89	0.46	25.89	0.46	-25.25	-26.56
$V_r \approx 1.0m/s$	55	±1.60	-27.36	0.71	27.36	0.71	-25.34	-28.06
$V_r \approx 1.5m/s$	29	±0.77	-26.66	0.26	26.66	0.26	-26.37	-27.53
$V_r \approx 2.0m/s$	7	±0.45	-27.59	0.26	27.59	0.26	-27.34	-27.93

Table 5.32: Refrigerant pressure loss: Analysis for ranges of refrigerant velocity

Condensed rate comparisons between the numerical and experimental results have been done in order to validate the capability of the numerical model to predict the latent cooling load of the tested heat exchanger. The numerical and experimental results, uncertainties, and the differences between them are presented in Table 5.33. A statistical analysis for all wet experimental points is presented in Table 5.34. The absolute average numerical to experimental difference for the data set of 71 wet cases is 10.12%, with standard deviation of 21.76%. As a whole, slight numerical over-prediction of the experimental results can be observed, but it is in the order of the experimental uncertainty. In some isolated cases the over-prediction reaches 133.43%. These are cases with very small condensed flow-rate (limit cases between dry and wet), and such large differences may also be due to the experimental error in the inlet air relative humidity measurement, or the condensate collection.

Case	$\dot{m}_{cond}^{num}$ $[\frac{kg}{h}]$	$\dot{m}_{cond}^{exp}$ $[\frac{kg}{h}]$	U_{cond} [%]	δ [%]
29	1.594	1.520	±5.263	4.85
30	2.196	2.170	±3.687	1.19
31	2.658	2.840	±2.817	-6.41
32	1.922	1.800	±4.444	6.77
33	2.914	2.650	±3.019	9.96
34	3.889	3.834	±1.956	1.44
35	0.603	0.561	±13.793	7.50
36	1.179	1.100	±7.273	7.18
37	1.884	1.760	±4.545	7.06
38	2.660	2.110	±3.791	26.07
39	3.402	3.120	±2.564	9.04
40	4.049	3.840	±2.083	5.45
41	4.846	4.600	±1.739	5.34
42	0.877	0.900	±8.602	-2.53
43	0.890	0.900	±8.602	-1.08
44	0.885	0.900	±8.602	-1.66
45	0.899	0.929	±8.333	-3.24
46	0.800	0.965	±10.811	-17.08
47	2.102	1.960	±4.082	7.25
48	3.904	3.590	±2.228	8.76
49	0.514	0.220	±36.364	133.43
50	0.822	0.856	±10.390	-3.97
...	...	...	...	...
99	5.634	5.130	±1.559	9.83

Table 5.33: Condensed rate: Numerical to experimental comparison

Zone	Points	$\bar{U}_{cond}$ [%]	$\bar{\delta}$ [%]	S_δ [%]	$\lvert\bar{\delta}\rvert$ [%]	$S_{\lvert\delta\rvert}$ [%]	Max [%]	Min [%]
Wet tests	71	±5.13	6.14	23.20	10.12	21.76	133.43	-19.53

Table 5.34: Condensed rate: Analysis for wet cases

Graphical comparisons have been plotted to facilitate the qualitative assessment of the numerical to experimental differences. In Figure 5.9 are presented the comparisons of the numerical and experimental data, given previously in tabular form.

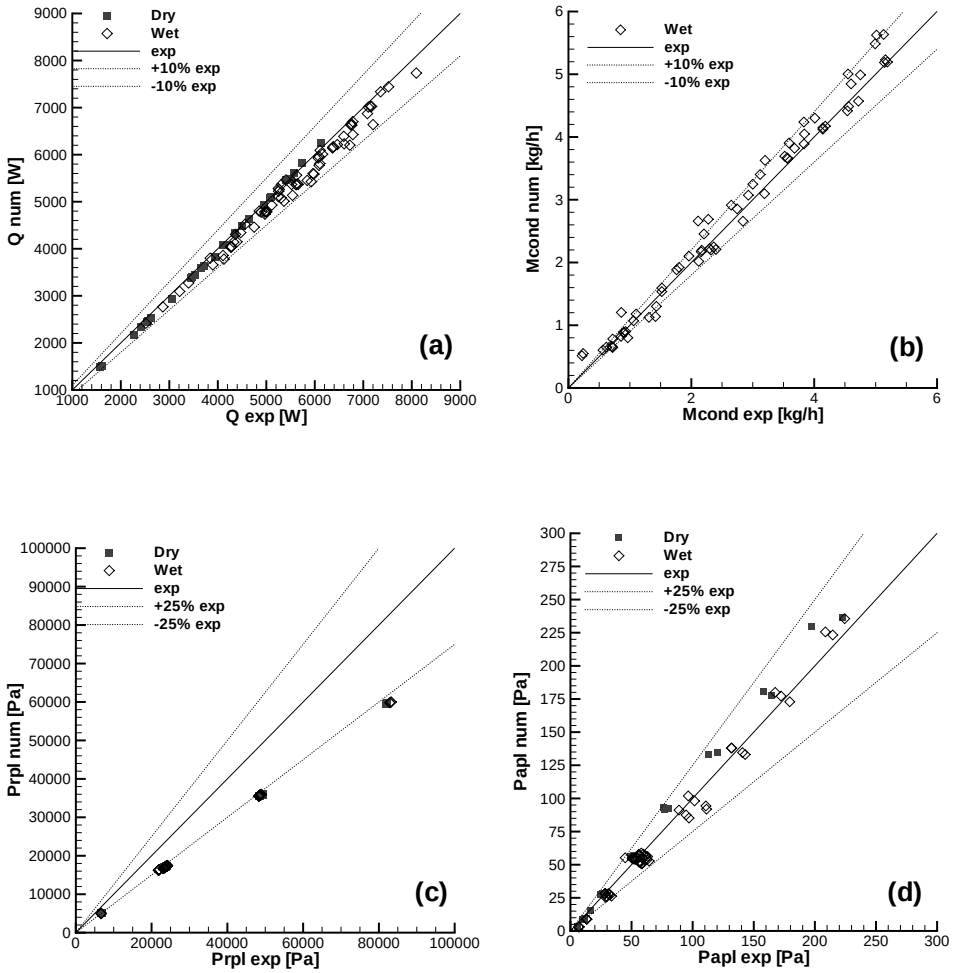

Figure 5.9: Graphical numerical to experimental comparison: (a) heat transfer capacity; (b) condensed flow; (c) refrigerant pressure loss; (d) air pressure loss.

5.5 Liquid overfeed refrigeration system

The liquid overfeed refrigeration system is designed and instrumented for experimental study of the refrigeration system and its components. More detailed information about the design, the system components and the measuring instrumentation is given in sections 3.4 and 3.5.3. The experimental system permits two modes of working. The first mode is experimentation with the vapour-compression liquid overfeed refrigeration system. The measurements in this mode are intended for validation of numerical models of the refrigeration system and its components (evaporator, condenser, compressor, etc.). The formulation used for determining the results of the measurements, as evaporator and condenser capacities, are presented in chapter 4, section 4.4. The evaluation of the measuring uncertainty and its propagation to the experimental results follows the methodology described in section 4.5. The second mode of working is for testing of the liquid overfeed evaporator without compressor. This has been possible with the implementation of a direct connection between the evaporator and the condenser in the liquid overfeed refrigeration system. The evaluation of the cooling capacity of the evaporator in this mode is based on the measurements of the secondary fluid in the condenser, as it is explained in section 4.4.3 (Testing of the evaporator without compressor).

5.5.1 Experimental results

The experimental measurements of the variables have been performed with the experimental facility operating continuously in a steady state regime, detected from the measurements of temperatures, absolute pressures and flow-rates of the primary and secondary refrigerants. As an indicator of the stable operation conditions has been taken also the stability of the liquid levels in the high- and low-pressure receivers.
In the experiments with the liquid overfeed refrigeration system, all the variables necessary for determining the refrigeration system operating point and the performance of the its basic components, are measured. On the primary refrigerant-side (R134a) the refrigerant temperatures at the inlet and outlet of the compressor, condenser and evaporator are measured. The absolute pressure of the refrigerant at the evaporator inlet, and the absolute pressures in the low- and high-pressure receivers are measured. The mass flow-rate of the refrigerant through the evaporator and the compressor are also measured. These experimental data in the primary refrigerant circuit (R134a) are presented in Table 5.35. The measured variables in the secondary fluids (air in the evaporator, and water in the condenser) are presented in Table 5.37.
In the tests of the liquid overfeed evaporator separately from the vapour-compression cycle (without compressor), the measured variables of relevance in the primary refrigerant circuit (R134a) are presented in Table 5.36. The measured variables in the air-side and the secondary fluid in the condenser are presented in Table 5.38.

Case	$\dot{m}_r$ $[\frac{kg}{h}]$	T_{ei} $[C]$	T_{eo} $[C]$	P_{ei} $[kPa]$	P_{rpl} $[Pa]$	T_{cdi} $[C]$	T_{cdo} $[C]$	P_{cd} $[kPa]$	T_{lpl} $[C]$	$\dot{m}_{cp}$ $[\frac{kg}{h}]$	T_{cpo} $[C]$
1	151.92	8.30	7.61	395.6	7790	71.84	55.30	1528.0	7.69	135.70	74.76
2	244.56	8.32	8.07	406.2	11270	71.84	55.47	1533.0	7.91	136.90	74.68
3	351.24	8.24	8.30	414.6	15430	71.83	55.47	1532.0	7.90	137.60	74.62
4	447.36	8.02	8.25	417.9	19360	71.87	55.59	1537.0	7.68	136.20	74.84
5	545.88	6.42	6.59	402.2	22120	72.07	55.33	1525.0	6.05	126.40	75.12
6	650.40	6.50	7.12	409.2	26740	72.12	55.36	1527.0	6.10	126.40	75.35
7	151.86	7.68	6.96	387.4	8719	66.32	48.88	1311.0	6.99	135.30	68.97
8	245.04	7.82	7.65	400.7	11990	66.36	49.12	1318.0	7.36	137.70	69.02
9	350.46	7.73	7.85	410.0	17310	65.96	49.10	1312.0	7.36	138.60	68.64
10	451.20	7.59	7.86	415.5	21300	65.84	48.99	1311.0	7.224	138.40	68.55
11	548.10	7.42	7.84	419.8	25650	65.81	48.95	1310.0	7.057	138.30	68.52
12	646.20	7.33	7.83	423.5	31250	65.79	49.01	1309.0	6.924	137.50	68.52
13	151.38	8.97	8.26	404.2	8672	66.25	49.35	1326.0	8.31	142.00	68.83
14	350.04	8.76	8.93	423.7	15900	66.18	49.15	1319.0	8.438	144.10	68.65
15	450.36	8.61	8.92	428.4	20250	66.19	49.12	1318.0	8.296	143.30	68.57
16	547.38	8.56	8.95	433.7	25760	66.24	49.12	1318.0	8.244	142.90	68.58
17	634.80	8.96	9.36	444.4	30920	66.65	49.25	1320.0	8.591	144.40	68.91
18	107.70	8.68	8.19	398.2	7499	70.82	55.10	1520.0	8.28	139.40	73.71
19	117.24	8.82	8.25	400.9	8769	70.82	55.04	1517.0	8.22	139.20	73.70
20	194.40	8.88	8.64	410.9	8526	70.77	55.09	1518.0	8.41	140.70	73.60
21	297.24	8.96	8.97	420.6	14060	70.79	55.11	1519.0	8.627	141.90	73.56
22	398.88	8.82	9.04	427.0	17680	71.08	55.38	1528.0	8.523	141.60	73.81
23	500.04	8.63	8.98	431.2	23490	71.06	55.37	1527.0	8.326	140.60	73.75
24	597.60	8.44	8.89	434.1	26660	70.97	55.29	1522.0	8.119	140.00	73.61

Table 5.35: Measured experimental results. Refrigerant R134a (refrig. cycle)

Case	$\dot{m}_r$ $[\frac{kg}{h}]$	T_{ei} $[C]$	T_{eo} $[C]$	P_{ei} $[kPa]$	P_{rpl} $[Pa]$	T_{cdi} $[C]$	T_{cdo} $[C]$	T_{lpl} $[C]$
1	201.78	8.58	9.89	427.2	5840	9.39	7.24	8.19
2	249.72	8.59	10.06	431.1	7408	9.47	7.35	8.25
3	300.84	8.61	10.22	435.4	9059	9.57	7.52	8.31
4	451.92	8.62	10.42	443.3	13890	9.55	7.66	8.34
5	552.66	8.61	10.52	447.8	16830	9.50	7.62	8.32
6	651.00	8.61	10.63	452.1	19440	9.47	7.55	8.28
7	202.68	9.09	10.36	434.9	6650	9.90	7.75	8.71
8	251.34	9.06	10.55	438.9	8199	10.03	7.97	8.74
9	300.72	9.09	10.74	443.0	9937	10.10	8.35	8.80
10	449.76	9.11	11.02	452.0	14950	10.13	8.31	8.85
11	560.52	9.07	11.13	457.0	18080	10.08	8.30	8.80
12	651.00	9.09	11.28	462.3	21060	10.11	8.06	8.79
13	167.16	9.54	10.75	438.4	6751	10.35	8.12	9.10
14	203.10	9.49	10.82	441.9	8090	10.38	8.10	9.10
15	252.00	9.49	11.02	447.1	9997	10.49	8.26	9.17
16	301.26	9.53	11.19	451.7	12070	10.58	8.43	9.24
17	459.66	9.48	11.41	461.4	18310	10.55	8.52	9.21
18	556.44	9.43	11.49	466.6	21660	10.51	8.48	9.16
19	646.80	9.45	11.65	471.9	24570	10.54	8.44	9.14

Table 5.36: Measured experimental results. Refrigerant (without compressor)

Case	$\dot{m}_a$ $[\frac{kg}{s}]$	T_{ai} $[C]$	T_{ao} $[C]$	φ_i [%]	φ_o [%]	P_{apl} $[Pa]$	$\dot{m}_{cds}$ $[\frac{kg}{h}]$	T_{cdsi} $[C]$	T_{cdso} $[C]$
1	0.4713	32.67	23.29	33.06	57.92	24.4	1217	50.28	54.77
2	0.4723	32.73	23.21	32.59	57.55	24.8	1217	50.38	54.91
3	0.4727	32.61	23.14	32.76	57.76	24.8	1219	50.36	54.89
4	0.4737	32.67	23.22	32.75	57.74	24.7	1215	50.53	55.04
5	0.4790	29.68	21.05	36.12	60.83	25.0	1216	50.55	54.80
6	0.4818	29.53	20.96	36.60	61.76	25.1	1216	50.59	54.85
7	0.7202	29.68	23.10	36.12	54.14	52.1	1235	43.86	48.47
8	0.7213	29.64	23.00	37.37	56.06	52.3	1235	43.97	48.68
9	0.7200	29.52	22.86	38.08	57.28	51.8	1238	43.78	48.50
10	0.7195	29.57	22.94	38.26	57.51	51.6	1239	43.75	48.46
11	0.7191	29.61	22.98	38.73	58.19	51.9	1237	43.77	48.47
12	0.7195	29.55	22.99	39.30	58.81	52.0	1237	43.76	48.43
13	0.9678	29.69	24.45	40.34	55.31	81.4	1235	44.07	48.89
14	0.9620	29.62	24.26	42.46	58.57	79.5	1236	43.80	48.68
15	0.9619	29.71	24.37	42.44	58.38	79.8	1237	43.79	48.64
16	0.9607	29.90	24.60	42.21	57.96	79.5	1237	43.79	48.65
17	0.9869	29.65	24.55	43.02	58.35	81.2	1235	43.84	48.73
18	0.7082	30.14	23.77	35.06	52.01	50.3	1217	49.94	54.52
19	0.7094	30.13	23.79	34.91	51.70	50.8	1216	49.87	54.45
20	0.7099	30.15	23.73	34.54	51.48	50.7	1218	49.85	54.47
21	0.7117	30.14	23.61	34.24	51.14	51.3	1218	49.81	54.47
22	0.7114	30.17	23.66	33.54	50.01	51.4	1218	50.10	54.73
23	0.7111	30.25	23.79	33.34	49.72	52.0	1218	50.11	54.70
24	0.7123	30.11	23.77	33.87	50.02	51.8	1219	50.07	54.60

Table 5.37: Measured experimental results. Secondary fluids (refrig. cycle)

Case	$\dot{m}_a$ $[\frac{kg}{s}]$	T_{ai} $[C]$	T_{ao} $[C]$	φ_i [%]	φ_o [%]	P_{apl} $[Pa]$	$\dot{m}_{cds}$ $[\frac{kg}{h}]$	T_{cdsi} $[C]$	T_{cdso} $[C]$
1	0.4714	30.14	22.42	33.07	52.97	25.0	1295	5.79	8.36
2	0.4714	30.15	22.34	33.53	53.80	24.8	1295	5.77	8.35
3	0.4709	30.16	22.34	33.62	54.08	25.5	1294	5.75	8.36
4	0.4705	30.19	22.44	33.91	54.33	25.6	1294	5.71	8.32
5	0.4700	30.19	22.51	34.46	54.91	24.1	1291	5.71	8.31
6	0.4703	30.18	22.58	34.98	55.44	24.9	1294	5.71	8.29
7	0.7201	30.19	24.46	33.85	48.05	53.0	1291	5.76	8.74
8	0.7207	30.21	24.47	32.78	46.68	51.5	1291	5.79	8.77
9	0.7214	30.19	24.42	32.91	46.82	52.4	1296	5.79	8.77
10	0.7210	30.20	24.49	32.62	46.33	52.6	1295	5.82	8.78
11	0.7209	30.18	24.55	32.84	46.37	52.0	1295	5.84	8.62
12	0.7199	30.25	24.71	33.14	46.79	51.9	1296	5.86	8.80
13	0.9577	30.10	25.32	35.45	47.84	78.8	1291	5.76	9.08
14	0.9575	30.19	25.28	34.56	46.99	79.1	1291	5.69	9.06
15	0.9571	30.19	25.21	34.25	46.56	78.6	1293	5.70	9.09
16	0.9589	30.20	25.21	33.36	45.50	79.3	1293	5.70	9.10
17	0.9573	30.19	25.26	32.29	43.76	79.1	1292	5.70	9.08
18	0.9580	30.18	25.32	31.42	42.46	80.1	1293	5.75	9.08
19	0.9578	30.24	25.39	31.72	42.74	80.3	1294	5.77	9.08

Table 5.38: Measured experimental results. Secondary fluids (without compressor)

5.5.2 Energy balance checks

The energy balance checks are an application of the energy conservation law to each one of the experiments. Energy balance checks have been done for the components of the refrigeration system where additional measurement of the same quantity exists. The obtained quantities from both measurements must agree within their uncertainty intervals.
The objective of the balance checks is two-fold. In the initial phase of the experiment they can help to determine if some errors in the measurements have not been taken into account. In the execution phase of the experiment balance checks help to control and verify the quality of the experimental results and detect possible failures in the instrumentation, or the process control.
The used measuring instrumentation permits the condenser capacity to be determined from the measurements in the primary refrigerant of the refrigeration cycle (R134a), and from the measurements in the secondary refrigerant fluid (water). The condenser capacities have been determined independently on the both sides using the formulation presented in section 4.4, and their uncertainties have been evaluated using the methodology presented in section 4.5. The results are presented Table 5.39. The relative difference between the capacities determined on the primary and secondary refrigerant-side is also presented, relative to the average condenser capacity. A qualitative comparison is presented in Figure 5.10.

Case	$\dot{Q}_{cd}$ [W]	U_{cd} [%]	$\dot{Q}_{cds}$ [W]	U_{cds} [%]	$100\frac{\lvert Q_{cd}-Q_{cds}}{0.5(\dot{Q}_{cd}+\dot{Q}_{cds})}$ [%]
1	6217	± 2.029	6353	± 2.711	2.18
2	6258	± 2.029	6410	± 2.690	2.41
3	6290	± 2.029	6421	± 2.690	2.06
4	6217	± 2.029	6371	± 2.701	2.45
5	5800	± 2.029	6009	± 2.844	3.53
6	5799	± 2.029	6023	± 2.838	3.78
7	6491	± 2.027	6619	± 2.650	1.95
8	6589	± 2.027	6763	± 2.602	2.61
9	6620	± 2.027	6794	± 2.597	2.59
10	6612	± 2.027	6785	± 2.602	2.57
11	6609	± 2.027	6760	± 2.607	2.25
12	6567	± 2.027	6716	± 2.621	2.24
13	6770	± 2.027	6921	± 2.551	2.21
14	6884	± 2.027	7013	± 2.525	1.85
15	6849	± 2.027	6975	± 2.538	1.82
16	6832	± 2.027	6990	± 2.534	2.28
17	6913	± 2.027	7021	± 2.521	1.56
18	6358	± 2.029	6481	± 2.665	1.91
19	6355	± 2.029	6475	± 2.665	1.88
20	6417	± 2.029	6543	± 2.645	1.94
21	6471	± 2.029	6599	± 2.626	1.97
22	6446	± 2.030	6557	± 2.640	1.70
23	6401	± 2.030	6500	± 2.660	1.53
24	6379	± 2.030	6421	± 2.690	0.65

Table 5.39: Condenser: Calculated results

The experimental set-up and the installed instrumentation permit balance check to be done for the liquid overfeed evaporator. This can be done for the two modes of working of the experimental facility with phase-changing refrigerant: vapour-compression system testing, and separate testing of the evaporator without compressor, comparing the cooling capacity determined refrigerant-side with that determined air-side. The cooling capacity of the evaporator refrigerant-side in the mode of vapour-compression system testing is determined from an energy balance over the low pressure receiver. The formulation used to determine the cooling capacity in this mode, and the vapour quality of the refrigerant at the outlet, is presented in section 4.4.3 (Testing of the evaporator as a part of the refrigeration cycle). The calculated experimental results for the evaporator, and their evaluated uncertainties are presented in Table 5.40. A qualitative representation of the cooling capacities determined refrigerant- and air-side with uncertainty intervals are showed in Figure 5.11.
The cooling capacity of the evaporator refrigerant-side in the mode of testing without compressor is determined indirectly from the measurement of the inlet and outlet temperatures and flow-rate of the secondary fluid in the condenser. The formulation used for calculation of the cooling capacity and the outlet vapour quality of the evaporator is presented in section 4.4.3 (Testing of the evaporator without compressor). The calculated experimental results and their uncertainties are presented in Table 5.41. The refrigerant- and air-side cooling capacities, with uncertainty intervals are presented in Figure 5.12.

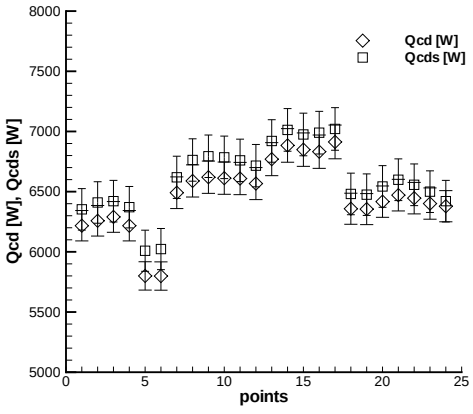

Figure 5.10: Condenser balance check

Case	V_a $[\frac{m}{s}]$	$\dot{Q}_a$ $[W]$	U_a [%]	$\dot{Q}_r$ $[W]$	U_r [%]	$\dot{Q}^*_{exp}$ $[W]$	U_{exp} [%]	x_g [%]	U_{x_g} [%]	$100\frac{\lvert\dot{Q}_a-\dot{Q}_r\rvert}{\dot{Q}_{exp}}$ [%]
1	2.09	4486	±5.55	4647	±1.06	4567	±3.01	57.60	±1.45	3.52
2	2.10	4559	±4.68	4692	±1.13	4626	±2.64	36.00	±1.50	2.87
3	2.10	4540	±4.64	4736	±1.22	4638	±2.62	25.06	±1.58	4.23
4	2.10	4538	±4.70	4660	±1.35	4599	±2.69	19.18	±1.68	2.65
5	2.10	4192	±4.87	4389	±1.52	4291	±2.80	14.50	±1.82	4.59
6	2.12	4185	±4.90	4351	±1.70	4268	±2.86	11.92	±2.01	3.89
7	3.17	4806	±6.10	4990	±1.06	4898	±3.47	61.72	±1.44	3.75
8	3.17	4855	±6.11	5073	±1.11	4964	±3.46	38.74	±1.48	4.39
9	3.17	4863	±7.53	5141	±1.18	5002	±4.05	27.21	±1.55	5.56
10	3.16	4838	±6.09	5104	±1.46	4971	±3.47	20.76	±1.79	5.35
11	3.16	4835	±6.19	5112	±1.41	4974	±3.50	16.93	±1.75	5.57
12	3.16	4789	±6.21	5079	±1.54	4934	±3.53	14.21	±1.86	5.88
13	4.27	5145	±7.31	5231	±1.05	5188	±4.23	65.23	±1.44	1.68
14	4.25	5234	±7.31	5336	±1.18	5285	±4.21	28.35	±1.55	1.93
15	4.25	5217	±7.45	5317	±1.28	5267	±4.28	21.76	±1.63	1.90
16	4.25	5168	±8.43	5316	±1.38	5242	±4.70	17.79	±1.72	2.82
17	4.36	5105	±7.59	5457	±1.46	5281	±4.30	15.73	±1.76	6.66
18	3.11	4572	±6.10	4805	±1.04	4689	±3.47	84.01	±1.43	4.97
19	3.12	4558	±6.18	4791	±1.04	4675	±3.51	77.06	±1.43	4.98
20	3.12	4621	±6.06	4843	±1.09	4732	±3.46	46.82	±1.47	4.69
21	3.13	4707	±6.08	4890	±1.16	4799	±3.47	30.82	±1.53	3.81
22	3.13	4691	±5.97	4862	±1.27	4776	±3.44	22.58	±1.62	3.58
23	3.13	4655	±6.26	4837	±1.39	4746	±3.58	17.79	±1.72	3.83
24	3.13	4576	±6.55	4847	±1.52	4711	±3.70	14.72	± 1.84	5.75
*	$\dot{Q}_{exp} = 0.5(\dot{Q}_a + \dot{Q}_r)$									

Table 5.40: Evaporator: Calculated results (refrigeration cycle)

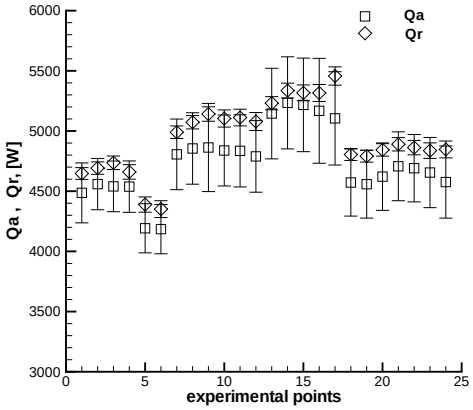

Figure 5.11: Evaporator balance check (refrigeration cycle)

Case	V_a $[\frac{m}{s}]$	$\dot{Q}_a$ $[W]$	U_a [%]	$\dot{Q}_r$ $[W]$	U_r [%]	$\dot{Q}^*_{exp}$ $[W]$	U_{exp} [%]	x_g [%]	U_{x_g} [%]	$100\frac{\lvert\dot{Q}_a-\dot{Q}_r\rvert}{\dot{Q}_{exp}}$ [%]
1	2.08	3688	±5.27	3660	±4.79	3674	±3.85	33.10	±5.09	0.76
2	2.08	3733	±5.39	3666	±4.79	3699	±3.89	26.47	±5.16	1.81
3	2.08	3733	±5.44	3722	±4.71	3727	±3.88	22.01	±5.17	0.30
4	2.08	3696	±5.19	3705	±4.73	3701	±3.80	13.97	±5.49	0.24
5	2.08	3656	±5.30	3686	±4.75	3671	±3.84	10.99	±5.75	0.81
6	2.08	3620	±5.28	3672	±4.77	3646	±3.85	8.96	±6.04	1.43
7	3.18	4182	±6.72	4263	±4.14	4222	±4.38	38.67	±4.39	1.92
8	3.18	4194	±6.65	4253	±4.15	4223	±4.36	30.75	±4.47	1.40
9	3.18	4217	±6.68	4273	±4.14	4245	±4.37	25.54	±4.53	1.32
10	3.17	4172	±6.74	4236	±4.17	4204	±4.40	16.29	±4.81	1.52
11	3.17	4113	±6.87	3975	±4.43	4044	±4.58	11.75	±5.35	3.41
12	3.17	4042	±7.26	4213	±4.20	4127	±4.60	10.48	±5.25	4.14
13	4.23	4640	±8.02	4773	±3.72	4707	±4.95	53.11	±3.94	2.82
14	4.23	4767	±8.16	4846	±3.67	4806	±4.99	44.08	±3.92	1.64
15	4.23	4831	±7.75	4893	±3.64	4862	±4.81	35.53	±3.94	1.27
16	4.24	4852	±7.70	4911	±3.63	4881	±4.79	29.54	±3.98	1.21
17	4.23	4782	±7.72	4854	±3.67	4818	±4.81	18.45	±4.22	1.49
18	4.23	4720	±7.79	4784	±3.72	4752	±4.87	14.60	±4.42	1.35
19	4.23	4703	±7.91	4768	±3.73	4736	±4.92	12.17	±4.61	1.37

* $\dot{Q}_{exp} = 0.5(\dot{Q}_a + \dot{Q}_r)$

Table 5.41: Evaporator: Calculated results (without compressor)

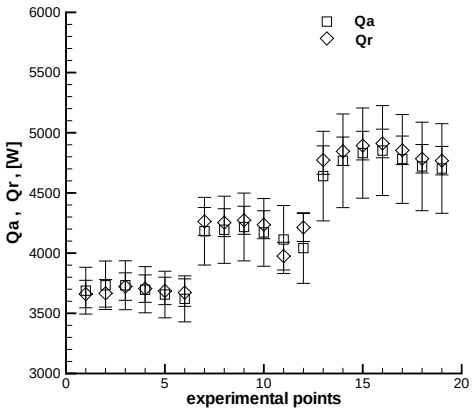

Figure 5.12: Evaporator balance check (without compressor)

The compressor work has been calculated from the experimental results. Just for comparison purposes, these measurements are contrasted to data supplied by the manufacturer, assuming a constant electrical-mechanical efficiency (see Figure 5.13).

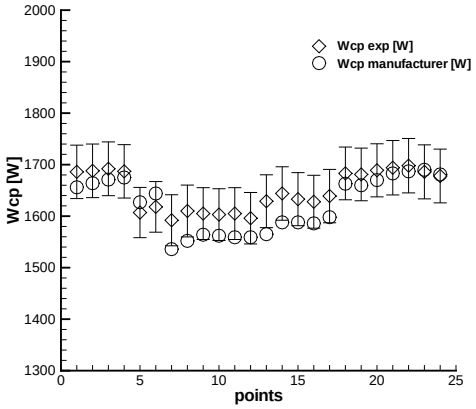

Figure 5.13: Compressor work

5.5.3 Validation methodology for the evaporator

An experimental validation methodology for the liquid overfeed evaporator is illustrated here with systematic comparisons of numerical and experimental results. The comparisons are carried out in three aspects in order to test the capabilities of the numerical model to predict the thermal and fluid-dynamic behaviour of the evaporator: cooling capacity, air pressure loss and refrigerant pressure loss. As the available experimental data contains only experimental cases in dry test conditions, the prediction comparisons of the latent cooling load over the evaporator have not been included. The same methodology can be used for more detailed studies, as the influence of different level of numerical model complexity, different experimental correlations, etc.
The numerically and experimentally determined cooling capacities and vapour qualities at the outlet of the evaporator are presented with their respective experimental uncertainties in tabular form. The numerical-experimental difference (δ) has been calculated from equation 5.3 and presented with the other data. The numerical to experimental comparisons for the evaporator from the tests with the refrigeration cycle are presented in Table 5.42. The comparisons of the results for the evaporator tested without compressor are presented in Table 5.43.

Case	$\dot{Q}_{num}$ [W]	$\dot{Q}_{exp}$ [W]	U_{exp} [%]	δ [%]	x_g^{num} [%]	x_g^{exp} [%]	U_{x_g} [%]	δ_{x_g} [%]
1	4344	4567	±3.01	-4.88	53.68	57.60	±1.45	-6.80
2	4291	4626	±2.64	-7.24	32.76	36.00	±1.50	-9.00
3	4216	4638	±2.62	-9.11	22.13	25.06	±1.58	-11.69
4	4242	4599	±2.69	-7.76	17.28	19.18	±1.68	-9.91
5	3971	4291	±2.80	-7.44	12.94	14.50	±1.82	-10.76
6	3863	4268	±2.86	-9.49	10.28	11.92	±2.01	-13.76
7	4733	4898	±3.47	-3.38	58.37	61.72	±1.44	-5.43
8	4623	4964	±3.46	-6.87	35.14	38.74	±1.48	-9.29
9	4511	5002	±4.05	-9.81	23.64	27.21	±1.55	-13.12
10	4505	4971	±3.47	-9.37	18.07	20.76	±1.79	-12.96
11	4485	4974	±3.50	-9.83	14.53	16.93	±1.75	-14.18
12	4467	4934	±3.53	-9.45	12.07	14.21	±1.86	-15.06
13	5074	5188	±4.23	-2.19	63.10	65.23	±1.44	-3.26
14	4960	5285	±4.21	-6.16	26.22	28.35	±1.55	-7.51
15	4983	5267	±4.28	-5.40	20.27	21.76	±1.63	-6.85
16	4989	5242	±4.70	-4.83	16.51	17.79	±1.72	-7.19
17	4767	5281	±4.30	-9.73	13.36	15.73	±1.76	-15.07
18	4424	4689	±3.47	-5.66	77.15	84.01	±1.43	-8.16
19	4435	4675	±3.51	-5.12	71.11	77.06	±1.43	-7.72
20	4417	4732	±3.46	-6.65	42.57	46.82	±1.47	-9.08
21	4361	4799	±3.47	-9.12	27.29	30.82	±1.53	-11.45
22	4333	4776	±3.44	-9.29	19.92	22.58	±1.62	-11.78
23	4344	4746	±3.57	-8.48	15.68	17.79	±1.72	-11.86
24	4356	4711	±3.70	-7.54	12.94	14.72	±1.84	-12.09

Table 5.42: Cooling Capacity: Num-exp. comparison (ref. cycle)

Case	$\dot{Q}_{num}$ [W]	$\dot{Q}_{exp}$ [W]	U_{exp} [%]	δ [%]	x_g^{num} [%]	x_g^{exp} [%]	U_{x_g} [%]	δ_{x_g} [%]
1	3361	3674	±3.85	-8.51	30.20	33.10	±5.09	-8.76
2	3350	3699	±3.89	-9.45	23.98	26.47	±5.16	-9.41
3	3324	3727	±3.88	-10.82	19.41	22.01	±5.17	-11.81
4	3352	3701	±3.80	-9.42	12.38	13.97	±5.49	-11.38
5	3354	3671	±3.84	-8.62	9.72	10.99	±5.75	-11.55
6	3318	3646	±3.85	-9.01	7.76	8.96	±6.04	-13.39
7	4024	4222	±4.38	-4.71	36.33	38.67	±4.39	-6.05
8	4017	4223	±4.36	-4.87	28.89	30.75	±4.47	-6.04
9	3991	4245	±4.37	-5.98	23.68	25.54	±4.53	-7.28
10	3967	4204	±4.40	-5.66	15.06	16.29	±4.81	-7.55
11	3916	4044	±4.58	-3.17	11.46	11.75	±5.35	-2.47
12	3935	4127	±4.60	-4.65	9.53	10.48	±5.25	-9.06
13	4426	4707	±4.95	-5.96	49.03	53.11	±3.94	-7.68
14	4447	4806	±4.99	-7.48	40.23	44.08	±3.92	-8.73
15	4412	4862	±4.81	-9.25	31.79	35.53	±3.94	-10.53
16	4385	4881	±4.79	-10.17	26.08	29.54	±3.98	-11.71
17	4315	4818	±4.81	-10.44	16.04	18.45	±4.22	-13.06
18	4281	4752	±4.87	-9.91	12.65	14.60	±4.42	-13.36
19	4292	4736	±4.92	-9.38	10.51	12.17	±4.61	-13.64

Table 5.43: Cooling Capacity: Num-exp. comparison (without compressor)

Points	$\bar{U}_{exp}$ [%]	$\bar{\delta}$ [%]	S_δ [%]	$\lvert\bar{\delta}\rvert$ [%]	$S_{\lvert\delta\rvert}$ [%]	Max [%]	Min [%]
24	±3.52	-7.28	2.20	7.28	2.20	-2.19	-9.83

Table 5.44: Cooling Capacity: Analysis for the whole data set (ref.cycle)

Points	$\bar{U}_{exp}$ [%]	$\bar{\delta}$ [%]	S_δ [%]	$\lvert\bar{\delta}\rvert$ [%]	$S_{\lvert\delta\rvert}$ [%]	Max [%]	Min [%]
19	±4.42	-7.76	2.35	7.76	2.35	-3.17	-10.82

Table 5.45: Cooling Capacity: Analysis for the whole data set (without compressor)

Zone	Points	$\bar{U}_{exp}$ [%]	$\bar{\delta}$ [%]	S_δ [%]	$\lvert\bar{\delta}\rvert$ [%]	$S_{\lvert\delta\rvert}$ [%]	Max [%]	Min [%]
$V_a \approx 2.0(m/s)$	6	±2.77	-7.65	1.64	7.65	1.64	-4.88	-9.49
$V_a \approx 3.0(m/s)$	13	±3.55	-7.73	2.07	7.73	2.07	-3.38	-9.83
$V_a \approx 4.0(m/s)$	5	±4.35	-5.66	2.72	5.66	2.72	-2.19	-9.73

Table 5.46: Cooling Capacity: Analysis for ranges of air velocity (ref.cycle)

Zone	Points	$\bar{U}_{exp}$ [%]	$\bar{\delta}$ [%]	S_δ [%]	$\lvert\bar{\delta}\rvert$ [%]	$S_{\lvert\delta\rvert}$ [%]	Max [%]	Min [%]
$V_a \approx 2.0(m/s)$	6	±3.85	-9.31	0.84	9.31	0.84	-8.51	-10.82
$V_a \approx 3.0(m/s)$	6	±4.45	-4.84	0.98	4.84	0.98	-3.17	-5.98
$V_a \approx 4.0(m/s)$	7	±4.88	-8.94	1.63	8.94	1.63	-5.96	-10.44

Table 5.47: Cooling Capacity: Analysis for ranges of air velocity (without compressor)

Zone	Points	$\bar{U}_{exp}$ [%]	$\bar{\delta}$ [%]	S_δ [%]	$\lvert\bar{\delta}\rvert$ [%]	$S_{\lvert\delta\rvert}$ [%]	Max [%]	Min [%]
$100 \leq \dot{m}_r(kg/h) < 200$	6	±3.53	-4.64	1.61	4.64	1.61	-2.19	-6.65
$200 \leq \dot{m}_r(kg/h) < 300$	3	±3.19	-7.74	1.20	7.74	1.20	-6.87	-9.12
$300 \leq \dot{m}_r(kg/h) < 400$	4	±3.58	-8.59	1.65	8.59	1.65	-6.16	-9.81
$400 \leq \dot{m}_r(kg/h) < 500$	3	±3.48	-7.51	1.99	7.51	1.99	-5.40	-9.37
$500 \leq \dot{m}_r(kg/h) < 600$	5	±3.66	-7.62	1.83	7.62	1.83	-4.83	-9.83
$600 \leq \dot{m}_r(kg/h) < 700$	3	±3.56	-9.56	0.15	9.56	0.15	-9.45	-9.73

Table 5.48: Cooling Capacity: Analysis for ranges of refrigerant flow (ref.cycle)

Zone	Points	$\bar{U}_{exp}$ [%]	$\bar{\delta}$ [%]	S_δ [%]	$\lvert\bar{\delta}\rvert$ [%]	$S_{\lvert\delta\rvert}$ [%]	Max [%]	Min [%]
$100 \leq \dot{m}_r(kg/h) < 200$	1	±4.95	-5.96	0.00	5.96	0.00	-5.96	-5.96
$200 \leq \dot{m}_r(kg/h) < 300$	6	±4.38	-7.38	2.12	7.38	2.12	-4.71	-9.45
$300 \leq \dot{m}_r(kg/h) < 400$	3	±4.34	-8.99	2.63	8.99	2.63	-5.98	-10.82
$400 \leq \dot{m}_r(kg/h) < 500$	3	±4.34	-8.51	2.52	8.51	2.52	-5.66	-10.44
$500 \leq \dot{m}_r(kg/h) < 600$	3	±4.43	-7.23	3.58	7.23	3.58	-3.17	-9.91
$600 \leq \dot{m}_r(kg/h) < 700$	3	±4.45	-7.68	2.63	7.68	2.63	-4.65	-9.38

Table 5.49: Cooling Capacity: Analysis for ranges of refrigerant flow (without compressor)

Statistical analyses have been carried out in order to determine the average numerical to experimental differences ($\bar{\delta}$) for the cooling capacity and their dispersions (S) for the compared cases. The analyses have been done for the whole data set and for groups of cases divided according to air velocity and refrigerant flow. This would show if some relation exists between the numerical-experimental differences and some specific working conditions. The results from the statistical analyses of the cooling capacity comparisons are presented in tabular form in Table 5.44 to Table 5.49.
In each table are presented the number of analysed test points, the average experimental uncertainty for the group of points ($\bar{U}_{exp}$), the average difference ($\bar{\delta}$), its dispersion (S_δ), the absolute value of the difference ($|\bar{\delta}|$) and its respective dispersion ($S_{|\delta|}$). In each table are presented also the minimum and maximum value of the difference found among all cases in the analysed group. For the groups of cases divided according to air velocity and refrigerant flow ranges, the corresponding zone is presented.
The cooling capacity differences are analysed first for the whole data set. The results for the tests with the refrigeration cycle are presented in Table 5.44 and the results from the tests without compressor are presented in Table 5.45. The average numerical to experimental differences ($|\bar{\delta}|$ are very similar for the both modes of testing and are respectively -7.28% and -7.76%, showing that the numerical model systematically under-predicts the cooling capacity of the evaporator. The differences are higher than the experimental uncertainties and therefore significative for the validation purpose.
The analyses for groups of air velocity and refrigerant flow-rate do not show any significant difference between the results for the considered groups in the experimentally studied range. As a whole the conclusion is that numerical model under-predicts the cooling capacity in the studied range up to approximately 10%.
The air pressure loss predictions of the numerical model are presented together with the experimentally measured values, the experimental measurement uncertainties, and the calculated numerical to experimental differences, for the refrigeration cycle experiments and for the experiments without compressor. The comparative results for the experiments with the refrigeration cycle are presented in Table 5.50. The results for the experiments without compressor are shown in Table 5.51. The measurement of the air pressure loss is practically not affected from the mode of testing of the evaporator (with the refrigeration system or without compressor), and differences can be expected only from the particular test conditions.
The statistical analyses for the air pressure loss are presented in Table 5.52 to Table 5.55. The presentation of the results is similar with that for the cooling capacity. The average experimental uncertainties for both modes are respectively ± 5.91 and ± 5.95, and the average numerical-experimental differences are 13.15% and 13.98% respectively, showing that the numerical model over-predicts the air pressure loss. The analysis for groups of air velocity reveals that the over-prediction is higher for the higher range of velocities, where the average differences come up to approximately

20% over-prediction.

Case	P_{apl}^{num} $[Pa]$	P_{apl}^{exp} $[Pa]$	U_{apl} [%]	δ [%]
1	27.9	24.4	±10.44	14.3
2	28.0	24.8	±10.27	12.8
3	28.0	24.8	±10.28	13.0
4	28.1	24.7	±10.31	13.6
5	28.6	25.0	±10.19	14.2
6	28.9	25.1	±10.15	15.1
7	57.6	52.1	±4.89	10.54
8	57.7	52.3	±4.87	10.36
9	57.5	51.8	±4.92	11.11
10	57.5	51.6	±4.94	11.3
11	57.4	51.9	±4.91	10.6
12	57.5	52.0	±4.90	10.4
13	95.9	81.4	±3.13	17.7
14	95.0	79.5	±3.21	19.4
15	95.0	79.8	±3.20	19.0
16	94.8	79.5	±3.21	19.2
17	99.3	81.2	±3.14	22.3
18	56.0	50.3	±5.07	11.3
19	56.1	50.8	±5.02	10.4
20	56.2	50.7	±5.03	10.9
21	56.5	51.3	±4.97	10.1
22	56.4	51.4	±4.96	9.76
23	56.4	52.0	±4.90	8.46
24	56.5	51.8	±4.92	9.16

Table 5.50: Air Pressure Loss: Num-exp. comparison (ref.cycle)

Case	P_{apl}^{num} $[Pa]$	P_{apl}^{exp} $[Pa]$	U_{apl} [%]	δ [%]
1	27.9	25.0	±10.19	11.40
2	27.9	24.8	±10.29	12.58
3	27.8	25.5	±10.00	9.16
4	27.8	25.6	±9.96	8.71
5	27.8	24.1	±10.59	15.31
6	27.8	24.9	±10.25	11.81
7	57.7	53.0	±4.81	8.94
8	57.8	51.5	±4.95	12.21
9	57.9	52.4	±4.87	10.44
10	57.8	52.6	±4.85	9.90
11	57.8	52.0	±4.90	11.08
12	57.7	51.9	±4.91	11.05
13	94.3	78.8	±3.24	19.77
14	94.3	79.1	±3.22	19.21
15	94.3	78.6	±3.24	19.97
16	94.6	79.3	±3.21	19.28
17	94.4	79.1	±3.22	19.31
18	94.5	80.1	±3.18	17.93
19	94.4	80.3	±3.18	17.64

Table 5.51: Air Pressure Loss: Num-exp. comparison (without compressor)

Points	$\bar{U}_{apl}$ [%]	$\bar{\delta}$ [%]	S_δ [%]	$\lvert\bar{\delta}\rvert$ [%]	$S_{\lvert\delta\rvert}$ [%]	Max [%]	Min [%]
24	±5.91	13.15	3.80	13.15	3.80	22.31	8.46

Table 5.52: Air Pressure Loss: Analysis for the whole data set (ref.cycle)

Points	$\bar{U}_{apl}$ [%]	$\bar{\delta}$ [%]	S_δ [%]	$\lvert\bar{\delta}\rvert$ [%]	$S_{\lvert\delta\rvert}$ [%]	Max [%]	Min [%]
19	±5.95	13.98	4.24	13.98	4.24	19.97	8.71

Table 5.53: Air Pressure Loss: Analysis for the whole data set (without compressor)

Zone	Points	$\bar{U}_{apl}$ [%]	$\bar{\delta}$ [%]	S_δ [%]	$\lvert\bar{\delta}\rvert$ [%]	$S_{\lvert\delta\rvert}$ [%]	Max [%]	Min [%]
$V_a \approx 2.0(m/s)$	6	±10.27	13.86	0.84	13.86	0.84	15.10	12.87
$V_a \approx 3.0(m/s)$	13	±4.95	10.36	0.83	10.36	0.83	11.35	8.46
$V_a \approx 4.0(m/s)$	5	±3.18	19.56	1.67	19.56	1.67	22.31	17.79

Table 5.54: Air Pressure Loss: Analysis for ranges of air velocity (ref.cycle)

Zone	Points	$\bar{U}_{apl}$ [%]	$\bar{\delta}$ [%]	S_δ [%]	$\lvert\bar{\delta}\rvert$ [%]	$S_{\lvert\delta\rvert}$ [%]	Max [%]	Min [%]
$V_a \approx 2.0(m/s)$	6	±10.21	11.50	2.41	11.50	2.41	15.31	8.71
$V_a \approx 3.0(m/s)$	6	±4.88	10.60	1.12	10.60	1.12	12.21	8.94
$V_a \approx 4.0(m/s)$	7	±3.21	19.02	0.89	19.02	0.89	19.97	17.64

Table 5.55: Air Pressure Loss: Analysis for ranges of air velocity (without compressor)

The numerical and the experimental refrigerant pressure losses through the evaporator are presented in Table 5.56 and Table 5.57, for the experimental points measured respectively with the refrigeration cycle and without compressor. The uncertainties in the experimental measurements (U_{rpl}) and the numerical-experimental differences (δ) are also presented. Statistical analyses for the numerical to experimental comparisons have been carried out. Summaries containing the average experimental uncertainties, average numerical to experimental differences, their dispersions, and the minimum and maximum differences among all compared points are presented in Table 5.58 and Table 5.59, for both modes of testing respectively. The numerical-experimental differences have been analyzed in groups for ranges of refrigerant flow-rate. The analyses show, that the numerical model as an average under-estimates the refrigerant pressure loss with 26.4% for the refrigerant cycle measurements, and 19.77% for the measurements in the working mode without compressor. In the lower range of refrigerant flow-rate

the numerical model gives predictions up to 75.4% lower than the experimental data for the cycle measurements, and up to 39.3% lower in the other mode, as can be seen in Table 5.60 and Table 5.61.

Case	P_{rpl}^{num} $[Pa]$	P_{rpl}^{exp} $[Pa]$	U_{rpl} [%]	δ [%]
1	4100	7790	±1.21	-47.37
2	8331	11270	±0.83	-26.08
3	12686	15430	±0.61	-17.78
4	16765	19360	±0.49	-13.41
5	19871	22120	±0.42	-10.17
6	22417	26740	±0.35	-16.17
7	4628	8719	±1.08	-46.92
8	9016	11990	±0.78	-24.80
9	13401	17310	±0.54	-22.58
10	17653	21300	±0.44	-17.12
11	21044	25650	±0.37	-17.96
12	24416	31250	±0.30	-21.87
13	4723	8672	±1.08	-45.53
14	14190	15900	±0.59	-10.75
15	18847	20250	±0.46	-6.93
16	22874	25760	±0.36	-11.20
17	24829	30920	±0.30	-19.70
18	1842	7499	±1.25	-75.44
19	2325	8769	±1.07	-73.48
20	6020	8526	±1.10	-29.40
21	10543	14060	±0.67	-25.01
22	14682	17680	±0.53	-16.96
23	18660	23490	±0.40	-20.56
24	22263	26660	±0.35	-16.49

Table 5.56: Ref.Pressure Loss: Num-exp. comparison (ref.cycle)

Case	P_{rpl}^{num} $[Pa]$	P_{rpl}^{exp} $[Pa]$	U_{rpl} [%]	δ [%]
1	4188	5840	±1.61	-28.28
2	5781	7408	±1.27	-21.96
3	7399	9059	±1.04	-18.33
4	11931	13890	±0.68	-14.10
5	14387	16830	±0.56	-14.52
6	16187	19440	±0.48	-16.73
7	5103	6650	±1.41	-23.27
8	6917	8199	±1.15	-15.64
9	8689	9937	±0.95	-12.56
10	13544	14950	±0.63	-9.41
11	16477	18080	±0.52	-8.86
12	18577	21060	±0.45	-11.79
13	4096	6751	±1.39	-39.33
14	5612	8090	±1.16	-30.64
15	7480	9997	±0.94	-25.18
16	9323	12070	±0.78	-22.76
17	14570	18310	±0.51	-20.43
18	17158	21660	±0.43	-20.78
19	19378	24570	±0.38	-21.13

Table 5.57: Ref.Pressure Loss: Num-exp. comparison (without compressor)

Points	$\bar{U}_{rpl}$ [%]	$\bar{\delta}$ [%]	S_δ [%]	$\lvert\bar{\delta}\rvert$ [%]	$S_{\lvert\delta\rvert}$ [%]	Max [%]	Min [%]
24	±0.65	-26.40	18.40	26.40	18.40	-6.93	-75.44

Table 5.58: Ref.Pressure Loss: Analysis for the whole data set (ref.cycle)

Points	$\bar{U}_{rpl}$ [%]	$\bar{\delta}$ [%]	S_δ [%]	$\lvert\bar{\delta}\rvert$ [%]	$S_{\lvert\delta\rvert}$ [%]	Max [%]	Min [%]
19	±0.86	-19.77	7.68	19.77	7.68	-8.86	-39.33

Table 5.59: Ref.Pressure Loss: Analysis for the whole data set (without compressor)

Zone	Points	$\bar{U}_{rpl}$ [%]	$\bar{\delta}$ [%]	S_δ [%]	$\lvert\bar{\delta}\rvert$ [%]	$S_{\lvert\delta\rvert}$ [%]	Max [%]	Min [%]
$100 \leq \dot{m}_r(kg/h) < 200$	6	±1.13	-53.02	17.91	53.02	17.91	-29.40	-75.44
$200 \leq \dot{m}_r(kg/h) < 300$	3	±0.76	-25.30	0.69	25.30	0.69	-24.80	-26.08
$300 \leq \dot{m}_r(kg/h) < 400$	4	±0.57	-17.02	4.86	17.02	4.86	-10.75	-22.58
$400 \leq \dot{m}_r(kg/h) < 500$	3	±0.46	-12.49	5.16	12.49	5.16	-6.93	-17.12
$500 \leq \dot{m}_r(kg/h) < 600$	5	±0.38	-15.28	4.45	15.28	4.45	-10.17	-20.56
$600 \leq \dot{m}_r(kg/h) < 700$	3	±0.25	-19.24	2.88	19.24	2.88	-16.17	-21.87

Table 5.60: Ref.Pressure Loss: Analysis for ranges of refrigerant flow (ref.cycle)

Zone	Points	$\bar{U}_{rpl}$ [%]	$\bar{\delta}$ [%]	S_δ [%]	$\lvert\bar{\delta}\rvert$ [%]	$S_{\lvert\delta\rvert}$ [%]	Max [%]	Min [%]
$100 \leq \dot{m}_r(kg/h) < 200$	1	±1.39	-39.33	0.00	39.33	0.00	-39.33	-39.33
$200 \leq \dot{m}_r(kg/h) < 300$	6	±1.26	-24.16	5.26	24.16	5.26	-15.64	-30.64
$300 \leq \dot{m}_r(kg/h) < 400$	3	±0.92	-17.88	5.12	17.88	5.12	-12.56	-22.76
$400 \leq \dot{m}_r(kg/h) < 500$	3	±0.61	-14.65	5.53	14.65	5.53	-9.41	-20.43
$500 \leq \dot{m}_r(kg/h) < 600$	3	±0.50	-14.72	5.96	14.72	5.96	-8.86	-20.78
$600 \leq \dot{m}_r(kg/h) < 700$	3	±0.44	-16.55	4.67	16.55	4.67	-11.79	-21.13

Table 5.61: Ref.Pressure Loss: Analysis for ranges of refrigerant flow (without compressor)

The above given numerical to experimental comparisons are presented in graphical form for visual qualitative evaluation. In Figure 5.14 and Figure 5.15 comparison of the experimentally and numerically determined cooling capacities is presented. The experimental results have been plotted in the abscissa and the numerical in the ordinate. In this way on the bisectrix would fall the cases in which the numerical and the experimental results coincide, above the bisectrix would fall the cases where the numerical model over-predicts the experimental result and below the bisectrix vice versa. Comparisons in the same style of the numerical to experimental air pressure loss are presented in Table 5.16 and Table 5.17. Refrigerant pressure drop comparisons are presented in Table 5.18 and Table 5.19 respectively for the refrigeration cycle experiment and the experiment without compressor.

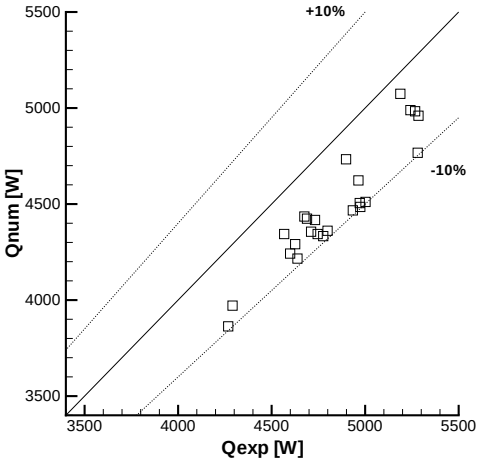

Figure 5.14: Comparison of experimental and numerical cooling capacities (refrigeration cycle)

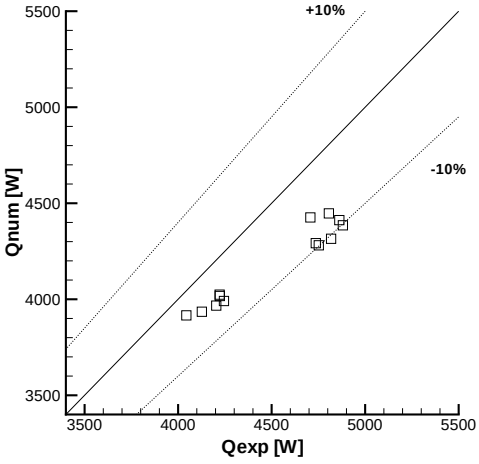

Figure 5.15: Comparison of experimental and numerical cooling capacity (without compressor)

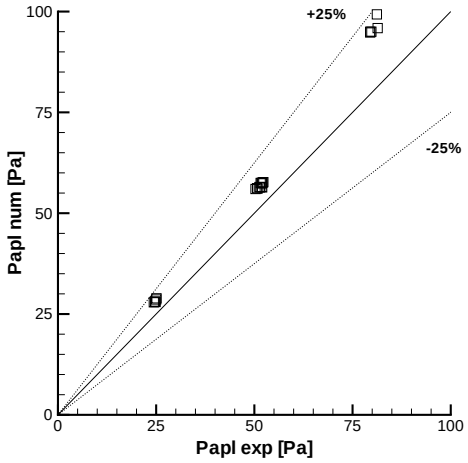

Figure 5.16: Comparison of experimental and numerical air pressure loss (refrigeration cycle)

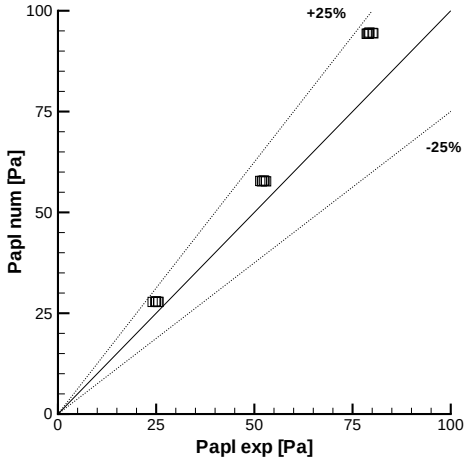

Figure 5.17: Comparison of experimental and numerical air pressure loss (without compressor)

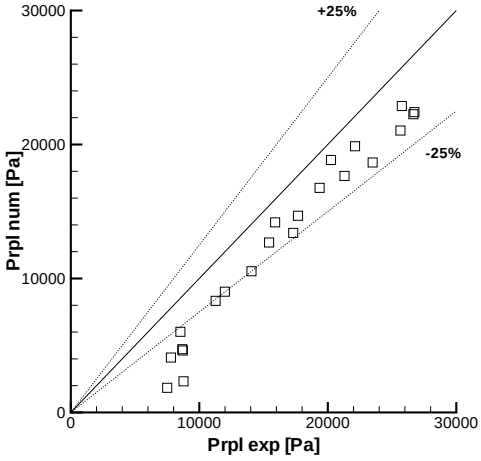

Figure 5.18: Comparison of experimental and numerical refrigerant pressure loss (refrigeration cycle)

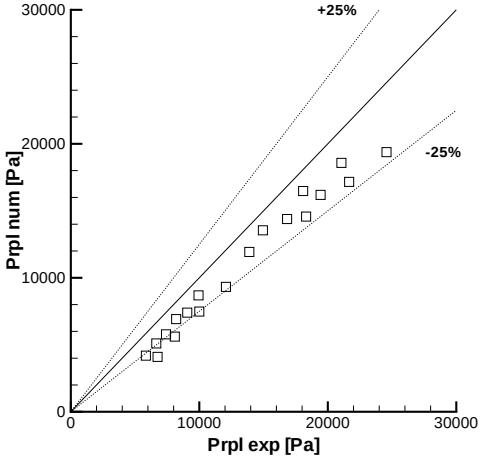

Figure 5.19: Comparison of experimental and numerical refrigerant pressure loss (without compressor)

5.6 Conclusions

In this chapter the results from the experimentation carried out with the developed infrastructure, and the comparative studies with results from mathematical models, aiming experimental validation, are presented. The experimental work comprises detailed studies of compact heat exchangers working as air-coolers in applications using liquid and phase-changing refrigerant, and studies with the experimental liquid overfeed refrigeration system.

Two prototypes of compact heat exchangers using water as a refrigerant have been prepared and tested in a wide range of air and refrigerant velocities, in dry and dehumidifying conditions. Detailed description of the prototypes' geometry and the experimental conditions is given, as to permit comparisons with results from mathematical models to be done in a straightforward and clear manner. In order to give more general use of the obtained experimental data the raw experimental values of the measured variables during the tests are presented in tabular form. The experimental cooling capacities and their uncertainties are determined from the measurements according to the methods described in chapter 4. The experimental results have been compared with results from the heat exchanger simulation model CHESS ([2], [3]), presented in chapter 2. A methodology for experimental validation of the mathematical models is proposed, based on systematic comparisons of numerical predictions and experimental results for the cooling capacity, the air and refrigerant pressure drops, and the latent cooling load.

An experimental study of the developed liquid overfeed refrigeration system has been carried out. Variables permitting the characterization of its operation and components have been measured throughout the system. The obtained results for the basic components of the system have been checked through energy balances from the available data in order to verify their correctness.

The liquid overfeed evaporator has been studied in detail in both testing modes described previously, calculating its cooling capacity under the test conditions following the formulation presented in section 4.4. The experimental uncertainty related with the determined cooling capacity has been estimated according the methodology presented in section 4.5. Numerical results for the liquid overfeed evaporator have been obtained using the CHESS compact heat exchanger simulation tool. An experimental validation methodology, similar as the applied for the compact heat exchangers using liquid refrigerant, has been presented, based on the available numerical and experimental data.

5.7 Nomenclature

$\dot{m}$	mass flow rate $[kg/s]$, $[kg/h]$
Max	maximum value of δ
Min	minimum value of δ
P	pressure $[Pa]$, $[kPa]$
$\dot{Q}$	cooling capacity $[W]$
S	sample standard deviation
T	temperature $[^oC]$
U	experimental uncertainty [%]
V	velocity $[m/s]$
x_g	refrigerant vapour quality

Greek symbols

δ	numerical to experimental difference
ϕ	generic variable
φ	air relative humidity [%]

Subscripts

a	air
ai	air inlet
ao	air outlet
apl	air pressure loss
cd	condenser
cdi	condenser inlet
cdo	condenser outlet
cds	condenser secondary fluid
$cdsi$	condenser secondary fluid inlet
$cdso$	condenser secondary fluid outlet
$cond$	condensed water
ei	evaporator inlet
eo	evaporator outlet
exp	experimental
i	inlet
lpl	low pressure receiver liquid
num	numerical
o	outlet
r	refrigerant
ri	refrigerant inlet
ro	refrigerant outlet
rpl	refrigerant pressure loss

x_g	refrigerant quality at evaporator outlet

Superscripts

exp	experimental
num	numerical

References

[1] Hugh W. Coleman and W. Glen Steele. *Experimentation and Uncertainty Analysis for Engineers*. John Wiley & Sons, 1989.

[2] Oliet C., Pérez-Segarra C.D., García-Valladares O., and Oliva A. Advanced Numerical Simulation of Compact Heat Exchangers. Application to Automative, Refrigeration and Air-Conditioning Industries. In *Proceedings of the European Congress on ComputationalMethods in Applied Sciences and Engineering (ECCOMAS)*, Barcelona, 2000.

[3] Oliet C., Pérez-Segarra C.D., Danov S., and Oliva A. Numerical Simulation of Dehumidifying Fin-and-tube Heat Exchangers. Model Strategies and Experimental Comparisons. In *Ninth International Refrigeration and Air Conditioning Conference at Purdue*, 2002.